ARTICLE

Adiponectin restrains ILC2 activation by AMPK-mediated feedback inhibition of IL-33 signaling

Lu Wang[1,3]*, Yan Luo[1,2]*, Liping Luo[1]*, Dandan Wu[1,4]*, Xiaofeng Ding[1], Handong Zheng[4], Haisha Wu[3], Bilian Liu[2], Xin Yang[1], Floyd Silva[1], Chunqing Wang[1], Xing Zhang[1], Xianyun Zheng[1], Jindong Chen[3], Jonathan Brigman[6], Michael Mandell[4,5], Zhiguang Zhou[2], Feng Liu[7], Xuexian O. Yang[4,5], and Meilian Liu[1,5]

ILC2s are present in adipose tissue and play a critical role in regulating adipose thermogenesis. However, the mechanisms underlying the activation of adipose-resident ILC2s remain poorly defined. Here, we show that IL-33, a potent ILC2 activator, stimulates phosphorylation of AMPK at Thr[172] via TAK1 in primary ILC2s, which provides a feedback mechanism to inhibit IL-33–induced NF-κB activation and IL-13 production. Treating ILC2s with adiponectin or an adiponectin receptor agonist (AdipoRon) activated AMPK and decreased IL-33–NF-κB signaling. AdipoRon also suppressed cold-induced thermogenic gene expression and energy expenditure in vivo. In contrast, adiponectin deficiency increased the ILC2 fraction and activation, leading to up-regulated thermogenic gene expression in adipose tissue of cold-exposed mice. ILC2 deficiency or blocking ILC2 function by neutralization of the IL-33 receptor with anti-ST2 diminished the suppressive effect of adiponectin on cold-induced adipose thermogenesis and energy expenditure. Taken together, our study reveals that adiponectin is a negative regulator of ILC2 function in adipose tissue via AMPK-mediated negative regulation of IL-33 signaling.

Introduction

Beige or brite adipocytes, which are enriched in subcutaneous fat such as inguinal fat, have high thermogenic capacity and have become a new therapeutic target for the treatment of obesity (Boström et al., 2012; Fisher et al., 2012; Petrovic et al., 2010). Group 2 innate lymphoid cells (ILC2s) were first discovered in the lymphoid structure associated with adipose tissues in the peritoneal cavity (Moro et al., 2010) and are activated by the epithelial cell–derived cytokines IL-33 and IL-25, as well as thymic stromal lympoiphoidin, in response to allergens (Cayrol and Girard, 2014; Koyasu and Moro, 2013; Licona-Limón et al., 2013). It was recently shown that ILC2s are present in murine and human adipose tissue and play a critical role in regulating beige adipocyte development, referred to as browning of white adipose tissue (WAT), by producing the opioid peptide methione-enkephalin (Penk) and the type 2 cytokines IL-5 and IL-13 (Moro et al., 2010; Lee et al., 2015; Brestoff et al., 2015). Moreover, decreased ILC2 population and response in adipose tissue were considered as conserved characteristics of obesity and its related diseases, such as atherosclerosis (Brestoff et al., 2015; Lee et al., 2015; Newland et al., 2017; Ding et al., 2016). In contrast, activation of ILC2s promotes WAT browning and acts to prevent obesity (Brestoff et al., 2015; Lee et al., 2015). However, how adipose-resident ILC2s are recruited and regulated is poorly understood.

IL-33 plays an essential role in the activation of ILC2s in adipose tissue, as well as in the lung and intestine (Brestoff et al., 2015; Lee et al., 2015). Adipose tissue contains relatively high amounts of IL-33 compared with the lung and spleen (Miller et al., 2010; Vasanthakumar et al., 2015; Zeyda et al., 2013). Multiple types of adipose tissue–residing cells, including endothelial cells, fibroblasts, and adipocytes themselves, produce IL-33 (Molofsky et al., 2015; Odegaard et al., 2016; Li et al., 2018). As a member of the IL-1 family, IL-33 binds to the IL-1 receptor–related protein ST2 coupling an IL-1RAcP (IL-1 receptor accessory

protein) unit, by which it promotes TGFβ-activated kinase 1 (TAK1) binding to TNF-receptor–associated factor 6 (TRAF6) and activates the canonical IκB kinases (IKKs) IKKα and IKKβ, leading to the phosphorylation and degradation of IκB, releasing NF-κB (Cao et al., 1996; Takaesu et al., 2000; Wang et al., 2001). Activated NF-κB promotes transcription of GATA binding protein 3 (GATA3), ST2, and consequently IL-5 and IL-13, leading to the activation of ILC2s and the type 2 immune response (Ali et al., 2011; Lloyd, 2010; Guo et al., 2012; Lee et al., 2015; Brestoff et al., 2015). Hypoxia-inducible factor α was recently found to suppress ST2 expression and ILC2 function by regulating the glycolytic enzyme pyruvate kinase M2 (Li et al., 2018). In addition, IL-33 was shown to induce the ILC2 function via the intercellular cell adhesion molecule 1 (ICAM-1)–mediated activation of ERK1/2 that stabilizes GATA3 (Lei et al., 2018). However, the feedback regulation of IL-33 signaling to control ILC2 activation remains largely unknown.

The energy sensor AMP-activated protein kinase (AMPK) is activated by a deficit in nutrients and stimulates cellular metabolic pathways such as glucose uptake and fatty acid oxidation (Long and Zierath, 2006). AMPK is a heterotrimeric protein and consists of a catalytic α subunit and regulatory β and γ subunits (Hardie, 2004; Carling, 2004; Long and Zierath, 2006). Each α, β, and γ subunit is encoded by its own genes (α1 and α2, β1 and β2, or γ1, γ2 and γ3, respectively; Hardie, 2004; Carling, 2004; Long and Zierath, 2006). The elevation of intracellular levels of AMP, as well as an increased ratio of AMP to ATP, due to nutrient deprivation activates AMPK allosterically, inducing phosphorylation of AMPK at Thr^{172}, within the activation domain of the α subunit, by liver kinase 1 (LKB1; Hardie, 2004; Carling, 2004; Long and Zierath, 2006). AMPK is also activated by calcium/calmodulin–dependent protein kinase kinase (CaMKK) when the intracellular Ca^{2+} level is elevated (Woods et al., 2005; Hawley et al., 2005). While it has been well established that AMPK controls systemic energy and glucose homeostasis in skeletal muscle, liver, adipose tissues, and pancreatic β cells, all of which are insulin-target or producing tissues (Hardie, 2004; Carling, 2004; Long and Zierath, 2006), little is known about whether AMPK also plays an important role in immune responses. Very recently, Blagih et al. (2015) showed that AMPK is a key regulator of T cell bioenergetics and viability and subsequent T cell–mediated adaptive immunity. Whether AMPK is critical for the activation and function of ILC2s remains elusive.

In the present study, we observed that AMPK is activated upon IL-33 treatment, and feedback inhibits IL-33–stimulated phosphorylation of IKKα/β and IκBα in ILC2s. Adiponectin treatment, via synergistic activation of AMPK, inhibits the IL-33–stimulated NF-κB pathway and IL-13 production in ILC2s. Adiponectin deficiency enhanced cold-induced thermogenic gene expression and energy expenditure, which was associated with decreased ILC2 apoptosis and increased cytokine production by ILC2s; the antithermogenic effects of adiponectin were diminished by ILC2 deficiency or blocking ILC2 function. These results demonstrate that adiponectin plays a critical role in regulating ILC2s and energy expenditure through an AMPK-dependent negative regulation of IL-33 signaling, a potential adverse effect of adiponectin-based therapeutics.

Results

Adiponectin inhibits IL-33 signaling via an AMPK-dependent mechanism in ILC2s

We recently showed that leptin, an adipokine, promotes proliferation and survival of proallergic ILC2s and production of type 2 cytokines in the lung (Zheng et al., 2018; Zheng et al., 2016). We asked if adiponectin, the most abundant adipokine, is involved in the regulation of ILC2 function and whether adiponectin–ILC2 communication (if it exists) occurs in the local adipose tissue. Using flow cytometry analysis, we found that both adiponectin receptor 1 (AdipoR1) and adiponectin receptor 2 (AdipoR2) were present in ILC2s, as well as in macrophages and adipocytes (Fig. 1 A and Fig. S1 A). As expected, treatment with 5 μg/ml adiponectin stimulated phosphorylation of AMPK at Thr^{172} in adipose-resident ILC2s (Fig. 1 B). Surprisingly, adiponectin treatment suppressed IL-33–induced production of IL-13 in the stromal vascular fraction (SVF) of WAT (Fig. 1 C). Consistent with this, treatment of adiponectin also suppressed IL-33–induced production of IL-13 in primary ILC2s (Fig. 1 D), suggesting an inhibitory effect of adiponectin on IL-33–stimulated ILC2 activation. In support of this, treatment with 10 μM adiponectin receptor agonist (AdipoRon) suppressed IL-33–induced phosphorylation of IKKα/β at $Ser^{176/180}$ and IκBα at $Ser^{32/36}$, two well-known kinases in NF-κB signaling, in ILC2s (Fig. 1, E and F). In addition, IL-33 activated AMPK, as indicated by the phosphorylation of acetyl-coenzyme A (acetyl-CoA) carboxylase, whereas AdipoRon treatment further enhanced AMPK activation and suppressed IL-33–stimulated phosphorylation of IKKα/β in primary differentiated type 2 helper T cells (Th2 cells; Fig. 1 G), a lymphoid cell type closely related to ILC2s with the ability to produce the type 2 cytokines IL-5 and IL-13 (Zhu, 2015). However, the suppressive effects of AdipoRon on phosphorylation of IKKα/β were attenuated by knockdown of AMPK in Th2 cells (Fig. 1 H). These results suggest that adiponectin inhibits ILC2 function via AMPK activation.

AMPK is activated by IL-33, and feedback inhibits IL-33–induced NF-κB signaling

To dissect the role of AMPK in IL-33 signaling, we treated primary Th2 cells with 10 ng/ml IL-33 at various time points. We found that IL-33 treatment stimulated phosphorylation of AMPK as well as IKKα/β (Fig. 2 A). IL-33 treatment also stimulated the phosphorylation of Unc-51-like autophagy-activating kinase 1 (ULK1) at Ser^{317} (Fig. 2 A), a site that is phosphorylated following AMPK activation. In addition, the phosphorylation of AMPK and IKKα/β occurred at 5 min and reached its peak at ~10 min upon IL-33 treatment (Fig. 2 A). Consistent with this, IL-33 treatment for 10 min stimulated phosphorylation of AMPK in adipose-resident ILC2s (Fig. 2 B), suggesting the activation of AMPK by IL-33 in ILC2s. To determine whether AMPK plays a role in regulating ILC2 function, we cotreated isolated ILC2s with IL-33 and compound C, an AMPK-specific inhibitor. Inhibiting AMPK enhanced IL-33–stimulated phosphorylation of IKKα/β in
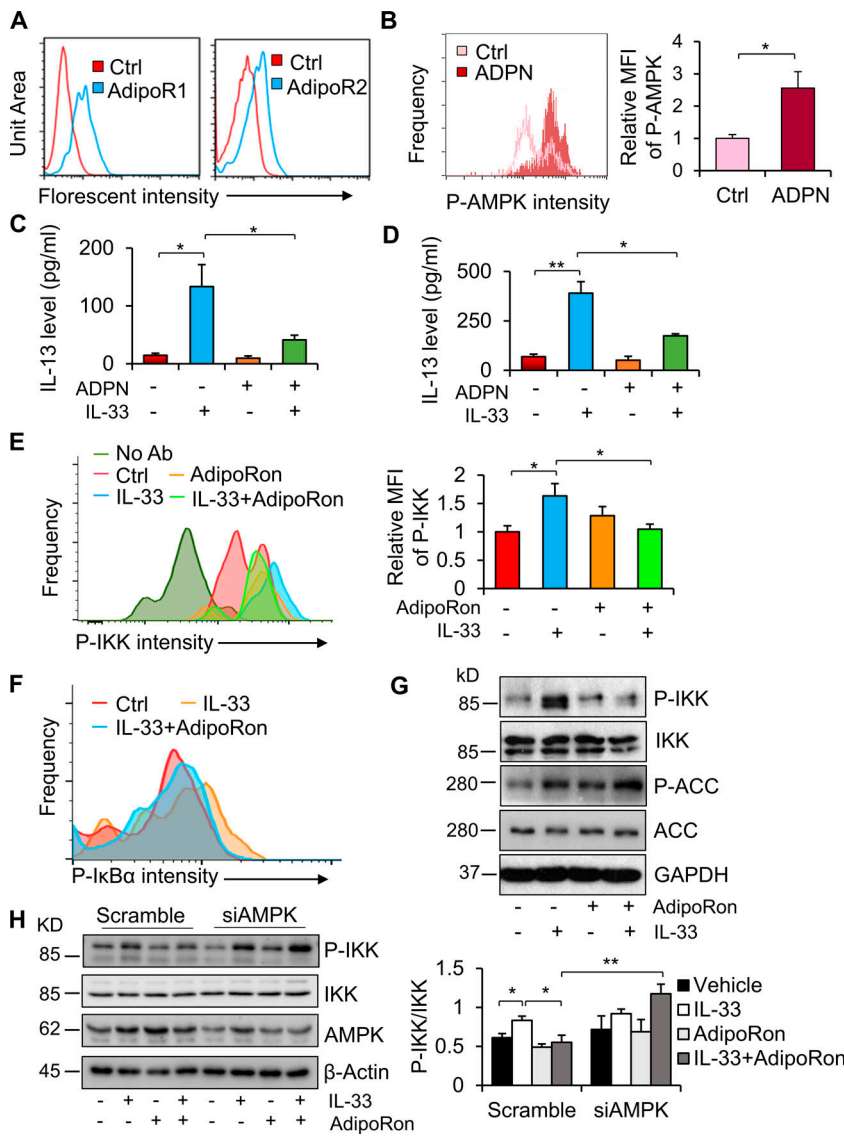
Figure 1. **Adiponectin inhibits IL-33 signaling in an AMPK-dependent manner in ILC2s.** Adipose-resident ILC2s were isolated from SVFs of WAT and cultured in a fresh RPMI medium with 1% FBS for 1 h for the following studies (A–F). **(A)** AdipoR1 and AdipoR2 were expressed in adipose-resident ILC2s. Two mice were used for each independent experiment. Representative data are presented from two independent experiments. **(B)** Adiponectin treatment stimulated AMPK phosphorylation in primary ILC2s. Starved cells were treated with 5 µg/ml full-length adiponectin for 20 min followed by flow cytometry analysis. ADPN, adiponectin. Three to six mice were used for each independent experiment. Data are shown as means ± SEM. *, P < 0.05, Student's t test. Each experiment was conducted three times independently. **(C)** Adiponectin treatment decreased the release of IL-13 induced by IL-33 in adipose SVF. SVFs were cultured in the medium containing 10% FBS and treated with 5 µg/ml full-length adiponectin for 1 h, followed by treatment with 10 ng/ml IL-33 for 18 h. The medium was collected for ELISA analysis. Three to six mice were used for each independent experiment. Data are presented as means ± SEM. *, P < 0.05, Student's t test. Each experiment was conducted three times independently. **(D)** Adiponectin treatment suppressed IL-33-induced IL-13 production in primary ILC2s. ILC2s were treated as described in C. Three to six mice were used for each independent experiment. Data are presented as means ± SEM. *, P < 0.05; **, P < 0.01, Student's t test. Each experiment was conducted three times independently. **(E and F)** Treatment with 10 µM AdipoRon suppressed IL-33-stimulated phosphorylation of IKKα/β (E) and IκBα (F). Starved ILC2s were treated with 10 µM AdipoRon for 1 h, followed by treatment with 10 ng/ml IL-33 for 10 min and flow cytometry analysis. Four to six mice were used for each independent experiment. Data are presented as means ± SEM. *, P < 0.05. Student's t test. Each experiment was conducted three times independently. **(G)** AdipoRon treatment suppressed IL-33-stimulated phosphorylation of IKKα/β in Th2 cells. One mouse was used for each independent experiment. Representative data are presented from three independent experiments. ACC, acetyl-CoA carboxylase; p-ACC, phosphorylation of acetyl-CoA carboxylase. **(H)** Suppressing AMPK by siRNA diminished the inhibitory effect of AdipoRon on IL-33-stimulated phosphorylation of IKKα/β in Th2 cells. Two mice were used for each independent experiment. Data are presented as means ± SEM. *, P < 0.05; **, P < 0.01; Student's t test. Each experiment was conducted three times independently. Ctrl, control; MFI, mean fluorescence intensity; No Ab, without treatment of antibodies; P, phosphorylation.

primary ILC2s (Fig. 2 C), indicating AMPK-mediated feedback inhibition of IL-33 signaling. Consistent with this, inhibiting AMPK increased IL-33-induced secretion of IL-13 in primary ILC2s, again suggesting a suppressive effect of AMPK on ILC2 function (Fig. 2 D). Moreover, compound C treatment or AMPK suppression enhanced IL-33-stimulated phosphorylation of IKKα/β in primary Th2 cells (Figs. 2 E and 1 H). To address how IL-33 activates AMPK, we blocked IL-1 receptor-associated kinase 1 (IRAK1) and TAK1 by pretreatment of Th2 cells with their specific inhibitors, IRAK1/4 inhibitor and 5Z-7-oxozeaenol (5Z), respectively. We found that inhibiting IRAK1 or TAK1 attenuated IL-33-stimulated phosphorylation of AMPK in Th2 cells (Fig. 2, F and G). Because TAK1 is downstream of IRAK1, we suppressed TAK1 using siRNA by electroporation in Th2 cells (Fig. 2 H). Suppressing TAK1 diminished IL-33-stimulated activation of AMPK in Th2 cells (Fig. 2 H), suggesting that TAK1 mediates the

activation of AMPK by IL-33. These results suggest that AMPK is activated upon IL-33 stimulation and that feedback inhibits IL-33-induced ILC2 activation.

Adiponectin deficiency enhances cold-induced ILC2 and type 2 immune responses in adipose tissue

Our results above suggest an important role of adiponectin in the negative control of IL-33-driven ILC2 responses. To determine the in vivo role of adiponectin in regulating ILC2s, we assessed ILC2 and other immune cell types in 10-wk-old adiponectin KO mice exposed to cold stress, a condition where ILC2s are activated (Lee et al., 2015; Brestoff et al., 2015). Despite a slight increase in ILC2 fraction in inguinal WAT (iWAT) at room temperature (22°C; Fig. S1 B), the frequency of ILC2s (CD45+Lin−CD90.2+ST2+ cells or CD45+Lin−CD90.2+RORC−ST2+GATA3+ cells) as well as M2 macrophages (CD206+/CD11b+), but not eosinophils

A

kD
62 — P-AMPK
62 — AMPK
85 — P-IKK
85 — IKK
150 — P-ULK1
140 — ULK1
45 — β-actin
(min) 0 5 10 15 30 60 IL-33

B

— IgG
— Ctrl
— IL-33

Frequency | P-AMPK intensity →

Relative MFI of P-AMPK
*
Ctrl   IL-33

C

— IgG   — IL-33
— Ctrl — Comp C
— IL-33 +Comp C

Frequency | P-IKK intensity →

Relative MFI of P-IKK
* * *
Comp C - - + +
IL-33   - + - +

D

IL-13 level (pg/ml)
450 300 150 0
** *
Comp C - - + +
IL-33   - + - +

E

kD
85 — P-IKK
85 — IKK
280 — P-ACC
280 — ACC
45 — β-Actin
Comp C - - + +
IL-33   - + - +

■Ctrl ☐IL-33 ■Comp C ☐Comp C+IL-33
P-protein/protein
P-IKK/IKK   P-ACC/ACC
* * **

F

kD
62 — P-AMPK
62 — AMPK
85 — P-IKK
85 — IKK
45 — β-Actin
IRAK1i - - + +
IL-33   - + - +

G

kD
62 — P-AMPK
62 — AMPK
85 — P-IKK
85 — IKK
5Z   - - + +
IL-33   - + - +

■Ctrl ☐IL-33 ■5Z ☐5Z+IL-33
P-protein/protein
P-AMPK/AMPK   P-IKK/IKK
* * * * * **

H

kD Scramble siTAK1
62 — P-AMPK
62 — AMPK
85 — P-IKK
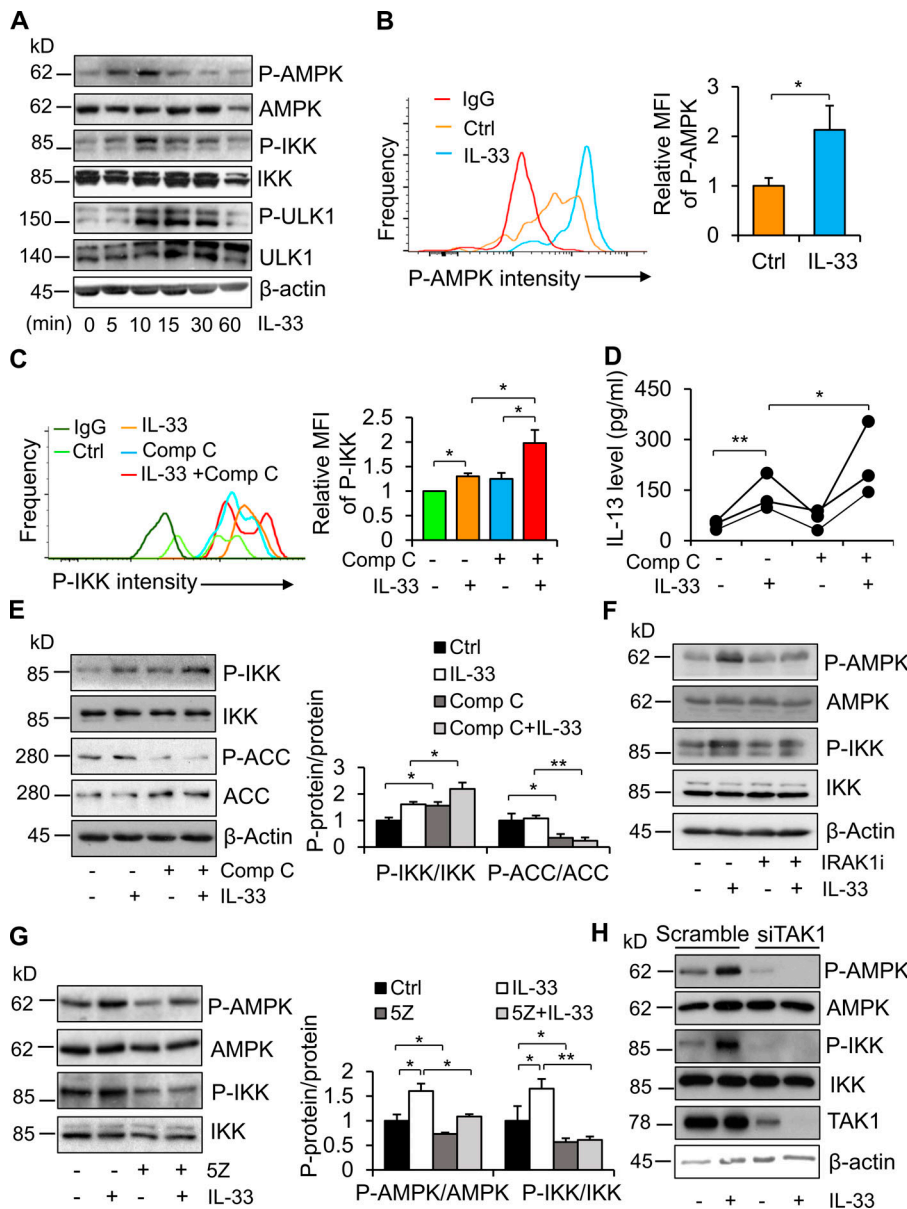85 — IKK
78 — TAK1
45 — β-actin
IL-33 - + - +

Figure 2. **AMPK is activated by IL-33, and feedback inhibits IL-33 signaling in ILC2. (A)** Phosphorylation of AMPK at Thr172 and ULK1 at Ser317, as well as phosphorylation of IKKα/β at Ser176/180, was stimulated by treatment with 10 ng/ml IL-33 in a time-dependent manner in primary differentiated Th2 cells. Cells were cultured in a fresh RPMI medium with 1% FBS for 1 h and then treated with 10 ng/ml IL-33 for 5, 10, 15, 30, and 60 min. Two mice were used for each independent experiment. Three times independently. **(B)** IL-33 treatment stimulated phosphorylation of AMPK at Thr172 in primary adipose-resident ILC2s. Three to four mice were used for each independent experiment. Data are presented as means ± SEM. *, P < 0.05, Student's t test. Each experiment was conducted three times independently. **(C)** Treatment with 1 μM compound C enhanced IL-33–stimulated phosphorylation of IKKα/β in primary ILC2s. Flow cytometry was used for the analysis of ILC2 in B and C. Four to six mice were used for each independent experiment. Data are presented as means ± SEM. *, P < 0.05, Student's t test. Each experiment was conducted three times independently. **(D)** Treatment of compound C elevated IL-33–induced secretion of IL-13 in primary ILC2s isolated for eWAT. Four to six mice were used for each independent experiment. *, P < 0.05; **, P < 0.01; Student's t test. Each experiment was conducted three times independently. **(E)** Inhibiting AMPK by treatment of 1 μM compound C increased IL-33–stimulated IKKα/β phosphorylation in Th2 cells. ACC, acetyl-CoA carboxylase; p-ACC, phosphorylation of acetyl-CoA carboxylase. One mouse was used for each independent experiment. Data are presented as means ± SEM. *, P < 0.05; **, P < 0.01; Student's t test. Each experiment was conducted three times independently. **(F and G)** Inhibiting IRAK1 (F) or inhibiting TAK1 (G) significantly suppressed IL-33–stimulated phosphorylation of AMPK in Th2 cells. Starved cells were treated with 10 μM IRAK1/4 inhibitor or 10 nM TAK1 inhibitor 5Z for 1 h, followed by treatment with 10 ng/ml IL-33 for 10 min. One mouse was used for each independent experiment. Data are presented as means ± SEM. *, P < 0.05; **, P < 0.01. Student's t test. Each experiment was conducted three times independently. **(H)** Suppressing TAK1 using siRNA alleviated IL-33–stimulated phosphorylation of AMPK and IKKα/β in Th2 cells. Starved cells were treated with 10 ng/ml IL-33 for 10 min. One mouse was used for each independent experiment. Each experiment was conducted three times independently. Ctrl, control; MFI, mean fluorescence intensity; P, phosphorylation.

(CD11b+Siglec-F+), in iWAT and epidydimal WAT (eWAT) was significantly increased by adiponectin deficiency under cold conditions (6°C for 48 h; Fig. 3, A and B; and Fig. S1, C and D). The fractions of ILC2, but not eosinophils and macrophages, were significantly increased by adiponectin deficiency in brown adipose tissue (BAT; Fig. 3, A and B; and Fig. S1, C and D). Moreover, adiponectin deficiency up-regulated basal and/or cold-induced expression of the type 2 cytokines IL-4 and IL-13 in iWAT and BAT despite an increase in IL-1, IL-10, and TNFα in iWAT as well as an increase in IL-1, IL-6, IL-10, and TNFα in BAT by adiponectin KO (Fig. 3 C and Fig. S1 E). Consistent with this, adiponectin deficiency led to an increase in the M2 macrophage markers CD206 and arginase 1 and the ILC2-derived factor Penk

in iWAT without significant effects on the macrophage marker F4/80 or the glucocorticoid receptor Nr3c1 (Fig. 3 D). In addition, adiponectin deficiency suppressed apoptosis of ILC2s despite no significant effect on proliferation (Figs. 3 E and Fig. S1 F). The inhibitory effect of adiponectin on ILC2 and Th2 cells was supported by the evidence of aggravated allergic asthma-stimulated ILC2/Th2 cell activation and type 2 immune response in the airways of adiponectin KO mice (Fig. S1, G–M).

Adiponectin deficiency enhances cold-induced thermogenesis and energy expenditure

Given the promoting effect of ILC2 on thermogenesis (Lee et al., 2015; Brestoff et al., 2015), we performed indirect calorimetry
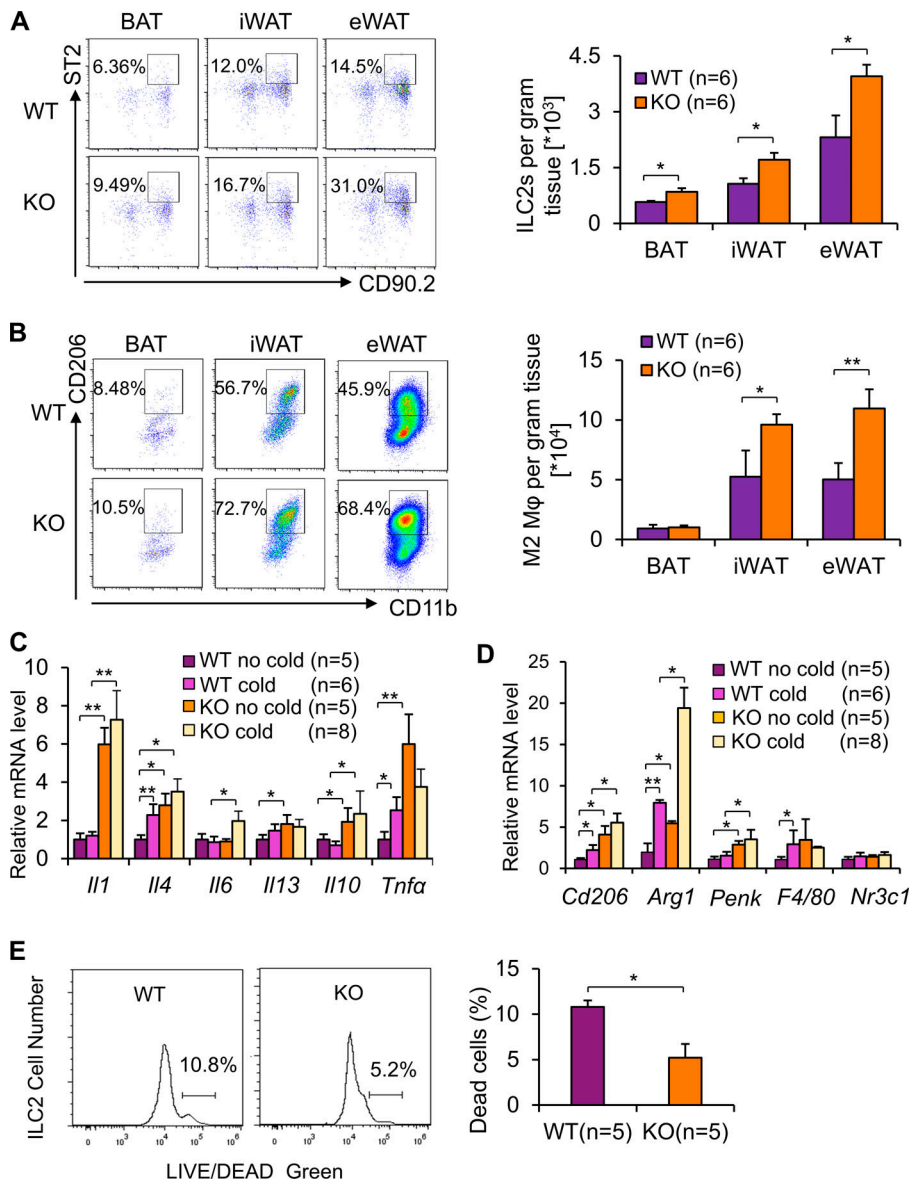
Figure 3. **Adiponectin deficiency increases adipose-resident ILC2 frequency and type 2 immune response.** For the following studies, 3-mo-old adiponectin KO and WT mice were exposed with or without cold stress (6°C) for 48 h. SVFs were isolated from iWAT, eWAT, and BAT; labeled by incubation with conjugated antibodies; and analyzed by flow cytometry. **(A and B)** Representative dot plots of ILC2s (CD45+Lin−CD90.2+ST2+; A) and M2 macrophages (CD206+/CD11b+; B) of brown (BAT), inguinal (iWAT), and epididymal (eWAT) fat pads from adiponectin KO and WT mice under cold stress condition. Statistical analysis of cell frequency was performed using the cell number per gram tissue. n = 6/group. Data are presented as means ± SEM. *, $P < 0.05$; **, $P < 0.01$; Student's t test. **(C)** Adiponectin deficiency up-regulated mRNA levels of IL-4 and IL-13 in iWAT under basal conditions. n = 5–8/group. Data are presented as means ± SEM. *, $P < 0.05$; **, $P < 0.01$; Student's t test. GAPDH was used as an internal control. **(D)** Basal and cold-induced mRNA levels of Penk and M2 macrophage markers were up-regulated in iWAT of adiponectin KO mice compared with the WT mice. n = 5–8/group. Data are presented as means ± SEM. *, $P < 0.05$; **, $P < 0.01$; Student's t test. **(E)** Adiponectin deficiency protected adipose-resident ILC2s from cell death induced by plate-bound anti-CD3 restimulation under room temperature conditions. n = 5/group. Data are presented as means ± SEM. *, $P < 0.05$; **, $P < 0.01$; Student's t test.

experiments in adiponectin KO mice. 10-wk-old male adiponectin KO and WT littermates were housed individually in the metabolic phenotyping system coupled with an environmental chamber. Adiponectin KO mice displayed slightly increased room temperature O$_2$ consumption throughout the light and dark cycle compared with WT littermates despite no significant differences in body mass, lean mass, fat mass, food intake, respiratory quotient, or beam-break counts (Fig. 4 A; and Fig. S2, A–D). This effect became more pronounced when the mice were exposed to both acute cold (6°C, for 48 h; Fig. 4 A) and chronic cold (6°C, for 6 d; Fig. 4 A). Consistently, adiponectin KO mice exhibited increased protein levels of the thermogenic markers UCP1, C/EBPβ, and PGC1α and mRNA levels of UCP1 and PGC1α in iWAT and BAT (Fig. 4, B–E; and Fig. S1 E). Furthermore, adiponectin deficiency protected mice from the cold stress–induced decline of core body temperature, with little effect on locomotor activity (Fig. 4 F and Fig. S2 E). Together, the results

from our study suggest that adiponectin exerts an antithermogenic effect.

Administration of AdipoRon inhibits ILC2 activation and cold-induced thermogenesis in adiponectin KO mice

To determine if adiponectin deficiency is the primary cause of increased energy expenditure and thermogenesis in adiponectin KO mice, we administered an adiponectin receptor agonist, AdipoRon, by i.p. injection to 10-wk-old adiponectin KO mice (Okada-Iwabu et al., 2013). AdipoRon administration for 5 d significantly decreased O$_2$ consumption while having little effect on food intake and activity under basal and cold stress conditions (Fig. 5 A; and Fig. S2, F and G). Moreover, the thermogenic markers UCP1, C/EBPβ, and PGC1α were suppressed by AdipoRon administration in iWAT, whereas the suppressive effects of AdipoRon in BAT were not significant (Fig. 5, B and C). In addition, the frequencies of ILC2s and M2 macrophages in iWAT were decreased by AdipoRon treatment under cold
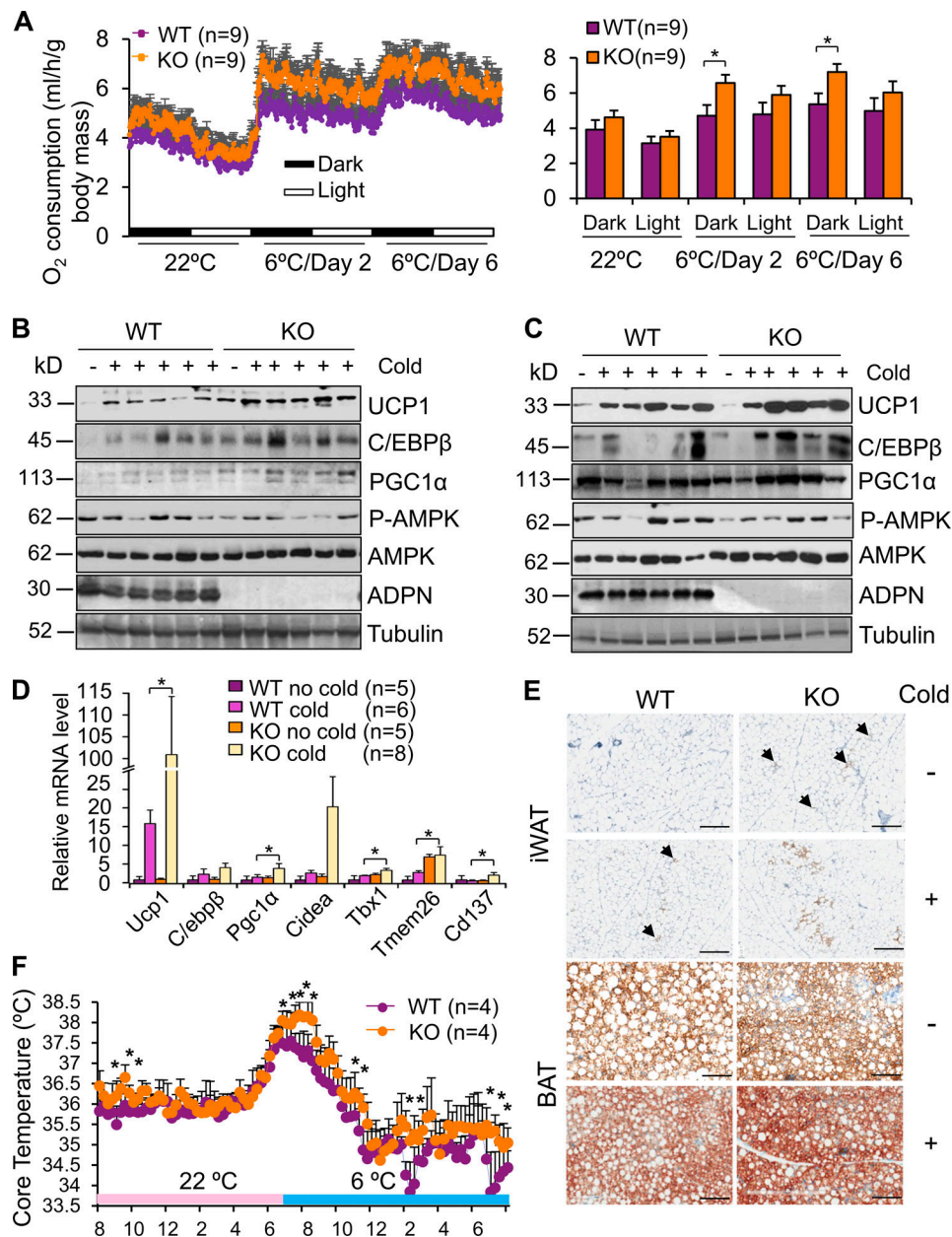
Figure 4. **Adiponectin deficiency increases energy expenditure and browning of WAT in vivo. (A)** Adiponectin KO mice displayed increased acute cold (6°C, for 48 h)– and chronic cold (6°C, for 6 d)–induced O_2 consumption throughout the light and dark cycle (n = 9/group). The average O_2 consumption was normalized to whole-body mass and analyzed by ANOVA. n = 9/group. Data are presented as means ± SEM. *, P < 0.05. **(B and C)** Cold (6°C, for 48 h)–induced expression levels of UCP1, C/EBPβ, and PGC1α were significantly up-regulated in iWAT (B) and slightly up-regulated in BAT (C) in adiponectin KO mice compared with WT mice. Representative data are presented. **(D)** The transcription of thermogenic genes and beige markers was up-regulated in adiponectin KO mice compared with WT mice under cold stress conditions. n = 5–8/group. Data are presented as means ± SEM. *, P < 0.05, Student's t test. **(E)** The staining of UCP1 in iWAT and BAT in the adiponectin KO and WT mice with/without cold stress. Arrowheads indicate UCP1+ beige adipocytes. Representative data are presented. Scale bars, 50 µm. **(F)** Adiponectin deficiency prevented a decline in body temperature in mice exposed to cold (6°C) in the feeding condition. n = 4/group. Data are presented as means ± SEM. *, P < 0.05, Student's t test. P-AMPK, phosphorylation of AMPK.

conditions (Fig. 5, D and E). In support of this, AdipoRon treatment decreased the fraction of eosinophils and total macrophages in iWAT, although the difference did not reach significance (Fig. S2, H and I). AdipoRon treatment also decreased the frequency of ILC2s and M2 macrophages in eWAT, while the difference did not reach significance accompanied with little effect on BAT (Fig. 5, D and E). However,

intracerebroventricular (i.c.v.) administration of trimeric adiponectin had no significant effect on energy expenditure, food intake, and activity (Fig. S2, J–L) or UCP1 expression in either BAT or iWAT (data not shown), indicating that the suppressive effect of adiponectin on cold adaptation is mediated at the level of periphery. In agreement with this, intra-iWAT injection of AdipoRon significantly suppressed cold-induced UCP1 expression
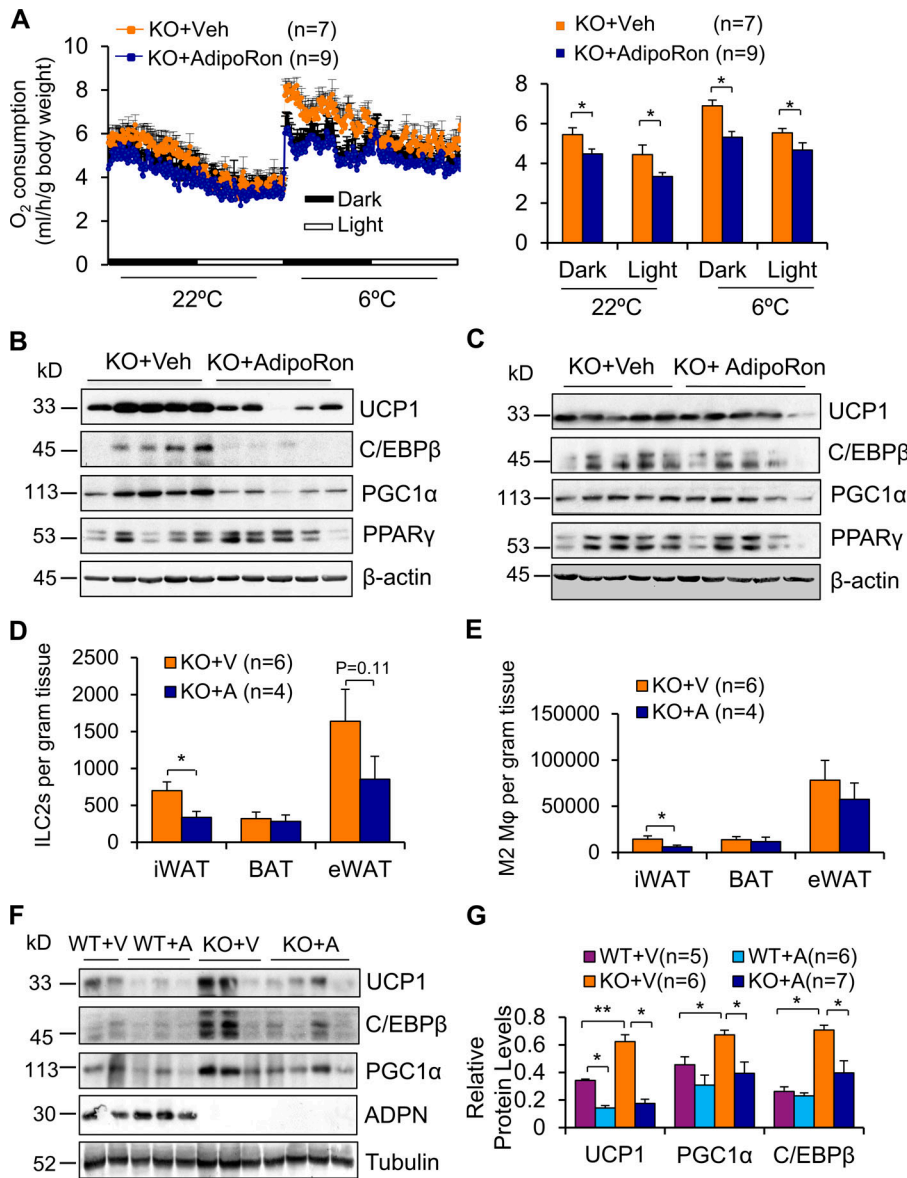
Figure 5. **AdipoRon administration suppresses ILC2 and energy expenditure in adiponectin KO mice. (A)** The effect of AdipoRon administration (30 mg/kg i.p. once per day for 5 d) on basal and cold-induced O_2 consumption in 10-wk-old adiponectin KO mice. 24 h after administration of AdipoRon, the calorimetry study was performed. The average O_2 consumption was normalized to whole-body mass and analyzed by ANOVA. n = 7–9/group. Data are presented as means ± SEM. *, P < 0.05. **(B and C)** Expression levels of UCP1, C/EBPβ, and PGC1α were significantly down-regulated by AdipoRon administration in iWAT (B) without significant difference in BAT (C) in adiponectin KO mice. Representative data are presented. **(D and E)** Administration of AdipoRon decreased the fractions of ILC2s (D) and M2 macrophages (E) in iWAT in adiponectin KO mice despite no significance in eWAT. n = 4–6/group. Data are presented as means ± SEM. *, P < 0.05, Student's t test. **(F)** Intra-iWAT injection of AdipoRon (3 mg/kg body mass) suppressed cold-induced expression of UCP1, C/EBPβ, and PGC1α in iWAT. Representative data are presented. **(G)** The data in F were quantified and analyzed. n = 5–7/group. Data are presented as means ± SEM. *, P < 0.05; **, P < 0.01; Student's t test. A, AdipoRon; V and Veh, vehicle.

(Fig. 5, F and G). Our data suggest that adiponectin plays a negative role in regulating energy expenditure via adipose tissue–dependent mechanisms.

Adiponectin inhibits cold-induced thermogenesis via ILC2-dependent mechanisms

To investigate if adiponectin suppresses adipose thermogenesis through regulating ILC2s, 10-wk-old adiponectin KO mice were administered ST2 antibody to neutralize IL-33 action as described (Fig. 6 A). Flow cytometry data show that administration of ST2/IL-1 R4 antibody significantly suppressed the fraction of ILC2s (Fig. 6 B). In addition, despite minor effects at room temperature, blocking ILC2 function diminished the increase of cold-induced O_2 consumption and up-regulation of the thermogenic genes *Ucp1*, *C/ebpβ*, and *Pgc1α* in iWAT in adiponectin KO mice under cold conditions (Fig. 6, C–E). Inhibiting ILC2 function, on the other hand, had little effect on food intake and activity (Fig. S2, M and N). Rag2/IL2rg double-KO mice were

known to lack ILC2s, and Rag2 KO mice were considered as ILC2-sufficient mice in previous studies (Brestoff et al., 2015). ILC2-deficient and sufficient mice were administered with AdipoRon. We observed that ILC2 deficiency diminished AdipoRon suppression of O_2 consumption and thermogenic gene expression in iWAT under both room temperature and cold stress conditions, indicating the mediatory role of ILC2s in adiponectin suppression of energy expenditure (Fig. 6, F and G). Moreover, the inhibitory effect of adiponectin on IL-4 and IL-13 production in the SVF was alleviated by ILC2 deficiency (Fig. 6, H and I), suggesting that adiponectin suppresses type 2 immune response and thermogenesis via ILC2-dependent mechanisms.

However, the role of adiponectin in the regulation of energy homeostasis and thermogenesis remains controversial in the field (Qi et al., 2004; Hui et al., 2015; Bauche et al., 2007; Masaki et al., 2003; Holland et al., 2013; Kubota et al., 2007; Kajimura et al., 2013; Qiao et al., 2014; Kim et al., 2007; Saito et al., 2006; Quaresma et al., 2016). To further address the controversy about
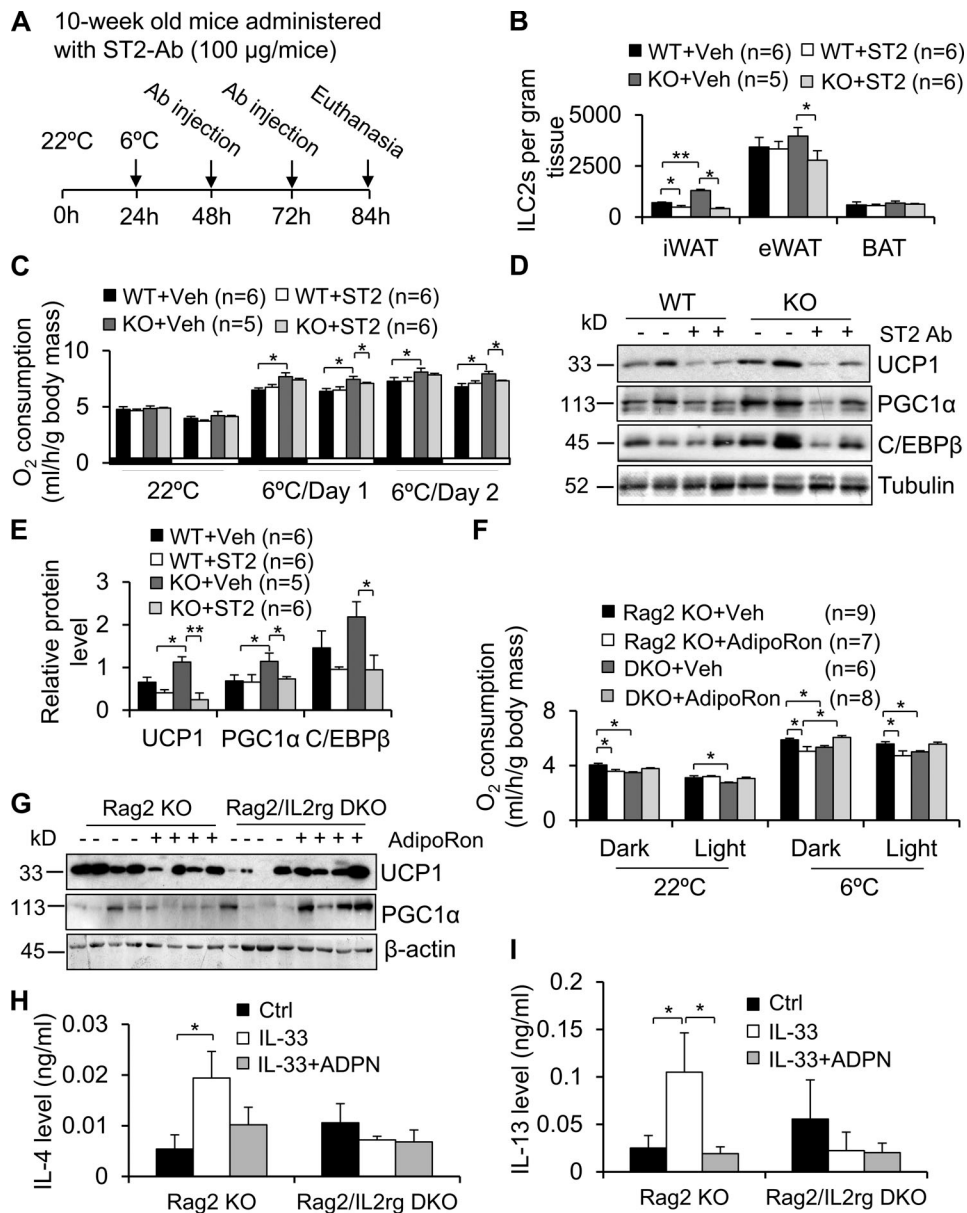
Figure 6. **Adiponectin negatively regulates thermogenesis via ILC2-dependent mechanisms. (A)** A time frame for administration of ST2 antibody in adiponectin KO and control mice. **(B)** Administration of ST2 antibody suppressed adiponectin deficiency–increased ILC2 fraction in iWAT and eWAT despite minor effects in BAT. n = 5–6/group. Data are presented as means ± SEM. *, $P < 0.05$; **, $P < 0.01$; Student's t test. **(C and D)** Blocking ILC2 function with ST2 antibody decreased adiponectin deficiency–increased O_2 consumption (C) and expression levels of thermogenic genes $Ucp1$, $C/ebp\beta$, and $Pgc1\alpha$ (D) under cold stress conditions. n = 5–6/group. Data are presented as means ± SEM. *, $P < 0.05$, Student's t test. **(E)** Expression levels of UCP1, C/EBPβ, and PGC1α in D were quantified and analyzed, and tubulin was used as a loading control. n = 5–6/group. Data are presented as means ± SEM. *, $P < 0.05$; **, $P < 0.01$. Student's t test. **(F and G)** The inhibitory effect of AdipoRon on O_2 consumption (F) and thermogenic gene expression in iWAT (G) was reversed by ILC2 deficiency. n = 6–9/group. Data are shown as means ± SEM. *, $P < 0.05$, Student's t test. **(H and I)** The secretion of IL-4 (H) and IL-13 (I) was enhanced by IL-33 and decreased by adiponectin treatment in the SVF of iWAT. SVF was cultured in FBS-free medium containing 0.5% BSA and then treated with or without 5 µg/ml adiponectin for 1 h, followed by treatment with or without 10 ng/ml IL-33 for 18 h using two mice for each independent experiment. Data are presented as means ± SEM. *, $P < 0.05$, Student's t test. Each experiment was conducted three times independently. ADPN, adiponectin; ST2, ST2 antibody; V and Veh, vehicle.

whether adiponectin exerts an antithermogenic effect, we ordered an additional mouse strain, in which adiponectin is also deficient, from Jackson Laboratory (B6;129-Adipoqtm1Chan/J, stock no. 008195; Adipo-; Ma et al., 2002). The mouse model from Jackson Laboratory has a B6;129 background, while the model used in the present study has a C57BL/6J background. Because the genetic background of strains has a considerable

impact on the metabolic phenotype (Hummel et al., 1972; Coleman and Hummel, 1973; Mao et al., 2006a; Fontaine and Davis, 2016), we backcrossed an adiponectin KO mouse model from Jackson Laboratory with C57BL/6J mice for four generations. As expected, adiponectin expression level was not detected in the KO mice, while it was highly enriched in adipose tissue of WT mice (Fig. S3, D and E). Using the same metabolic

phenotyping system for the present study, we found that O$_2$ consumption and thermogenic gene expression in iWAT and BAT were enhanced by adiponectin KO under cold stress conditions despite no significant difference on activity and food intake (6°C, 48 h; Fig. S3, A–E), confirming the antithermogenic function of adiponectin (Fig. 4). In addition, expression levels of ILC2 markers *St2* and *Penk* in iWAT and BAT, as well as ILC2 populations in iWAT, were significantly increased by adiponectin deficiency, although the difference in ILC2 population in BAT and *Il5* expression in iWAT and BAT did not reach significance (Fig. S3, F–H).

Cold stress suppresses expression levels and circulation levels of adiponectin in mice

Next, we investigated whether expression and circulating levels of adiponectin are affected by cold stress. 3-mo-old male C57BL/6 mice were housed in an environmental chamber either at 22°C or 6°C for 48 h. Cold exposure induced expression of UCP1 but down-regulated adiponectin expression in BAT and iWAT (Fig. 7, A and B), as well as circulating levels, in vivo (Fig. 7 C). Consistent with other recent studies (Hui et al., 2015; Dong et al., 2013), the circulating levels of adiponectin were also down-regulated by chronic cold stress (6°C, 6 d; Fig. 7 D), suggesting that adiponectin levels are negatively correlated with thermogenesis. Moreover, mRNA levels of adiponectin were suppressed by 2-d and 6-d cold stress in iWAT (Fig. 7, E and F). These results suggest that the levels of adiponectin in adipose tissue and in circulation are associated with cold adaptation.

Discussion

ILC2s were recently shown to be present in adipose tissue and play a critical role in regulating browning of WAT by promoting IL-4/IL-13–driven type 2 immunity or increasing the ILC2-derived cytokine Penk (Lee et al., 2015; Brestoff et al., 2015). Moreover, increased ILC2 response limits the development of obesity (Lee et al., 2015; Brestoff et al., 2015). However, the mechanisms underlying the activation of adipose-resident ILC2s remain largely unknown. Our present study shows that AMPK is downstream of IL-33 signaling and that feedback inhibits IL-33–induced activation of NF-κB and production of IL-13 in adipose-resident ILC2s. In addition, adiponectin suppresses cold-induced ILC2 activation through AMPK-mediated feedback inhibition of IL-33 signaling and subsequently suppresses thermogenic gene expression in adipose tissue and energy expenditure. Our results reveal a new mechanism underlying ILC2 activation and subsequent WAT browning in response to cold stress and also provides new insight into the proadipogenic effects of adiponectin.

IL-33 is an activator of ILC2s and plays a pivotal role in regulating metabolism (Lee et al., 2015; Brestoff et al., 2015). Moreover, a shorter, soluble version of IL-33 also has a direct impact on adipocytes by splicing *Ucp1* transcripts in the nucleus and regulating thermogenesis (Odegaard et al., 2016). IL-33 appears to be produced in adipose tissue, where fibroblasts are the main IL-33–producing cells (Kolodin et al., 2015; Kuswanto et al., 2016). Our laboratory and others have shown that IL-33 is
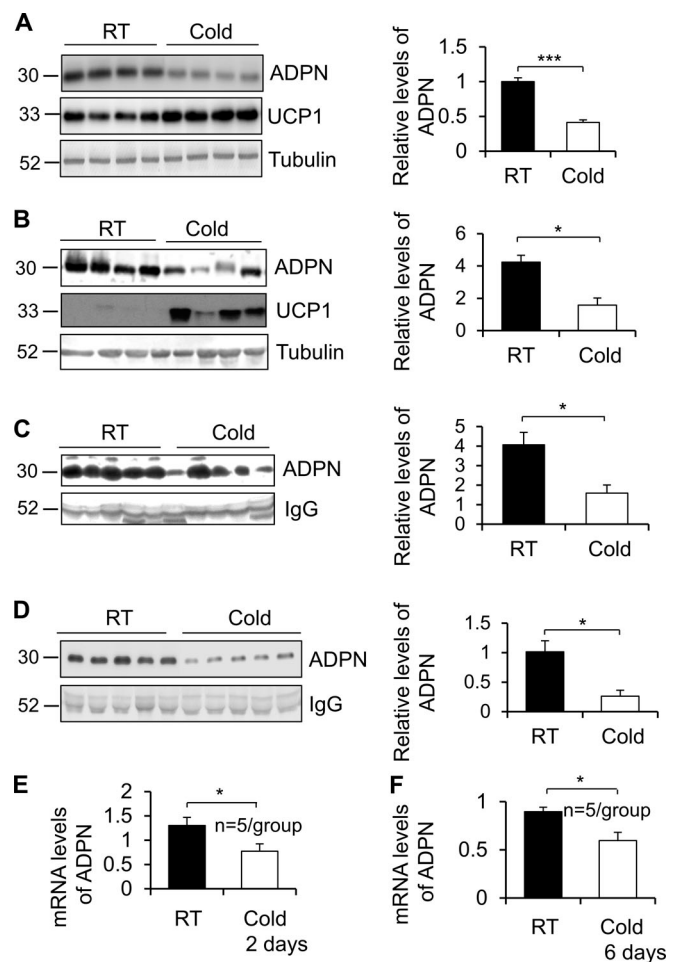

Figure 7. **Adiponectin levels are down-regulated by cold stress. (A and B)** The expression of adiponectin was down-regulated while expression of UCP1 was up-regulated by cold stress (6°C for 48 h) in BAT (A) and iWAT (B) of mice. n = 4/group. Data are presented as means ± SEM. *, P < 0.05; ***, P < 0.001; Student's t test. **(C and D)** The circulating levels of adiponectin were decreased by acute cold stress (6°C for 48 h; C) and chronic cold stress (6°C for 6 d; D). n = 5/group. Data are presented as means ± SEM. *, P < 0.05, Student's t test. **(E and F)** The mRNA levels of adiponectin were suppressed by acute cold stress (6°C for 48 h; E) and chronic cold stress (6°C for 6 d; F). n = 5/group. Data are presented as means ± SEM. *, P < 0.05, Student's t test. ADPN, adiponectin; RT, room temperature.

associated with cold adaptation and obesity development (Odegaard et al., 2016; Ding et al., 2016). However, little is known about the regulation of IL-33 signaling in ILC2s. We show that similar to IKKα/β, IL-33–stimulated AMPK is also inhibited by suppressing TAK1 in ILC2s (Fig. 2), indicating that TAK1 mediates IL-33–stimulated AMPK activation in ILC2s. In agreement with this, TAK1 was identified as a potential upstream kinase of the budding yeast orthologue of AMPK (the SNF1 complex) in yeast and phosphorylates Thr[172], activating AMPK in vitro (Momcilovic et al., 2006). In addition, TAK1 also mediates AMPK activation in response to various stimuli, including TNF-related apoptosis-inducing ligand, hydrogen peroxide, IL-1β, TNFα, and bacterial infection in epithelial cells and cardiomyocytes (Herrero-Martín et al., 2009; Chen et al., 2013; Liu et al., 2018; Xie et al., 2006; Antonia and Baldwin, 2018).

Activation of AMPK by TNF-related apoptosis-inducing ligand requires TAK1, but not LKB1 and CaMKK-β, the known upstream kinases for AMPK activation under conditions such as glucose starvation and calcium ionophore (Herrero-Martín et al., 2009; Xie et al., 2006). In support of this, our data suggest that TAK1 is required for IL-33–stimulated AMPK in ILC2s. Furthermore, Antonia and Baldwin (2018) showed that IKK directly phosphorylates AMPK at Thr^{172} when its own Thr^{172} is phosphorylated by TAK1, upon treatment of IL-1β or TNFα in cancer cells. Which kinase, TAK1 or IKK, catalyzes phosphorylation of AMPK may stem from the difference in cell types or stimuli. On the other hand, although IL-33 is a potent activator of ILC2, it may display opposite functions in ILC2s under various physiological conditions. Of note, IL-33 up-regulates PD-1 expression and intrinsically negatively regulates production of IL-5 and IL-13 on ILC2s in obese mice (Oldenhove et al., 2018). Given that TNFα-mediated M1 macrophage polarization is required for ILC2 dysfunction in obesity (Oldenhove et al., 2018), IL-33 up-regulation itself may be not sufficient to promote development as well as activation of ILC2 in adipose tissue under obese conditions.

AMPK activation provides a negative regulatory mechanism in IL-33 signaling in ILC2s and Th2 cells. Inhibiting or suppressing AMPK increases IL-33–induced ILC2 activation by enhancing the NF-κB pathway and secretion of IL-13 (Fig. 2). In support of this, both AdipoR1 and AdipoR2 are expressed in primary ILC2s, and adiponectin signaling suppressed the IL-33–stimulated NF-κB pathway in both Th2 cells and ILC2s (Fig. 1). This is also supported by the finding that adiponectin has been shown to inactivate NF-κB in other cell types (Ajuwon and Spurlock, 2005). We show that AMPK, a well-known effector of adiponectin signaling (Petrovic et al., 2010; Yamauchi et al., 2002; Wu et al., 2003; Mao et al., 2006b; Ruan and Dong, 2016), is critical for the inhibitory effect of adiponectin on IL-33–induced activation of IKK and IL-13 production in ILC2s, providing new insight into adiponectin inhibition of ILC2 function. However, how AMPK signaling inhibits NF-κB pathway in ILC2s remains poorly understood. Following AMPK activation, phosphorylation of ULK1 at Ser^{317}, an activation site of ULK1 and a marker of autophagy initiation, occurs in response to IL-33 treatment (Fig. 2 A). It is possible that AMPK/autophagy pathway inactivates NF-κB through regulating P62, given that P62 has been suggested to promote NF-κB through multiple mechanisms: increasing the phosphorylation of IKKβ by binding to atypical PKCs, activation and polyubiquitination of TRAF6, and promoting ROS-induced RAS expression (Lallena et al., 1999; Martin et al., 2006; Wooten et al., 2005; Duran et al., 2008). Future studies will be needed to clarify this possibility.

Adiponectin exerts antidiabetic effects (Ahima, 2006; Scherer, 2006; Kadowaki and Yamauchi, 2005; Kuswanto et al., 2016; Nawrocki et al., 2006), and its expression and circulating levels are down-regulated by obesity in human subjects (Scherer et al., 1995; Abbasi et al., 2004). However, the role of adiponectin in the regulation of energy homeostasis and thermogenesis remains controversial. Several studies show that adiponectin promotes energy expenditure and the cold-induced browning effect through its central and peripheral actions (Qi et al., 2004;

Hui et al., 2015; Bauche et al., 2007; Masaki et al., 2003; Holland et al., 2013). However, other studies have suggested that adiponectin may be a negative regulator of energy expenditure and thermogenesis (Kubota et al., 2007; Kajimura et al., 2013; Qiao et al., 2014; Kim et al., 2007; Saito et al., 2006; Quaresma et al., 2016). These inconsistent observations highlight the need for research identifying the true physiological functions and underlying mechanisms of adiponectin in the regulation of energy metabolism. In addition, there is also a controversy as to whether adiponectin acts as an anti- or proinflammatory mediator (Maeda et al., 2002; Xu et al., 2003; Kumada et al., 2004; Ohashi et al., 2010; Tsao et al., 2002; Cheng et al., 2012; Park et al., 2007; Awazawa et al., 2011; Tang et al., 2007; Ding et al., 2016). More importantly, it remains largely unknown whether adiponectin regulates thermogenesis and energy expenditure through an inflammatory response, which is a key factor of WAT browning (Molofsky et al., 2013; Lee et al., 2015; Qiu et al., 2014; Rao et al., 2014). By using adiponectin KO mice, Hui et al. (2015) found that adiponectin promotes WAT browning by direct stimulation of M2 macrophage proliferation, with little effect on ILC2s. This mouse model was shown to display a rather moderate phenotype in insulin sensitivity (Ma et al., 2002). By using the adiponectin KO mice that displayed magnified insulin resistance compared with the controls, when dietarily challenged (Nawrocki et al., 2006), we found that adiponectin plays an inhibitory role in regulating adipose-resident ILC2s, type 2 immunity, and energy expenditure (Figs. 2, 3, 4, and 5), suggesting that the inhibitory effect of adiponectin on thermogenesis may explain its proadipogenic properties.

To validate if adiponectin exerts antithermogenic effects, we ordered another adiponectin KO mouse strain from Jackson Laboratory and backcrossed this strain of adiponectin-deficient mice with C57BL/6 for four generations. The results also demonstrate that adiponectin acts as a negative regulator of ILC2s as well as thermogenesis in adipose tissue (Fig. S3). Using the same metabolic phenotyping system, we were the first to characterize two adiponectin KO mouse strains and show that adiponectin suppresses ILC2 function and thermogenesis. In support of this, Kajimura et al. (2013) generated one more adiponectin KO mouse model with a mixed background of C57BL/6J and 129/Sv and showed that adiponectin deficiency enhanced energy expenditure through the central nervous system. In contrast, administration of adiponectin receptor agonist AdipoRon reverses the increase in ILC2 population as well as energy expenditure in adiponectin KO mice under cold stress conditions (Fig. 5). Collectively, adiponectin-based therapeutics may bring potential side effects such as antithermogenic and pro-obesity effects.

On the other hand, it was recently challenged whether alternatively activated macrophages synthetize catecholamine or contribute to thermogenesis and energy homeostasis (Fischer et al., 2017). In addition, there is also a controversy regarding whether IL-4–IL-13 signaling plays an essential role in catecholamine production and thermogenesis (Fischer et al., 2017; Molofsky et al., 2013; Rao et al., 2014; Brestoff et al., 2015). Therefore, it remains unknown whether adiponectin suppresses cold-induced thermogenesis though the IL-4–IL-13 pathway and alternative activation of macrophage, two well-known pathways

downstream of ILC2 (Ding et al., 2016). Because expression levels of Penk are up-regulated by adiponectin deficiency in adipose tissue (Fig. 3 D), future studies will be needed to address whether Penk and IL-4–IL-13 pathways mediate the suppressive effect of adiponectin on thermogenesis. Up-regulation of leptin may also contribute to the defensive effect against obesity via ILC2 activation, given that leptin promotes the proliferation and activity of ILC2s in lung (Zheng et al., 2016; Zheng et al., 2018). In support of this, although adiponectin deficiency does not appear to overtly alter insulin sensitivity under normal chow diet conditions (Ma et al., 2002; Maeda et al., 2002), adiponectin has been reported to boost appetite, slow energy metabolism, and promote adipogenesis, all of which are well-defined factors promoting obesity development (Kubota et al., 2007; Kajimura et al., 2013; Kim et al., 2007). Similar to administration of per-oxisome proliferator–activated protein γ agonists thiazolidine-diones that improve insulin sensitivity but lead to severe obesity (Savage et al., 2003; Ristow et al., 1998), our study suggests that adiponectin-based treatment may bring the unfavorable effect of inducing obesity through inhibition of energy expenditure.

In summary, our study demonstrates that AMPK plays a critical role in regulating ILC2 function and adipose thermo-genesis. AMPK interacts with the NF-κB pathway by serving as a target of TAK1 and a feedback regulator of downstream path-ways of TAK1, such as IKKα/β and IκBα in ILC2s. Adiponectin suppresses ILC2 function via the AMPK pathway in vitro and in vivo. Cold stress down-regulates adiponectin, which alleviates AMPK-mediated feedback inhibition of IL-33 signaling and subsequently activates adipose-resident ILC2s and promotes adipose type 2 immune responses and thermogenesis. There-fore, our results reveal that adiponectin is a negative regulator of ILC2s through AMPK-dependent feedback inhibition of IL-33 signaling and that adiponectin exerts antithermogenic effects.

Materials and methods
Materials
Antibodies against phospho-AMPK (2531) at Thr^{172}, AMPK (2603), phospho-IKKα (Ser^{176})/IKKβ (Ser^{177}; 2078S), IKKα (2682), IKKβ (2370), phospho-IκB at Ser$^{32/36}$ (9246), IκB (4814), phospho-ULK1 at Ser^{317} (6887), and ULK1 (8054) were from Cell Signaling. Anti-PGC1α (ST1204) was purchased from Millipore. Antibodies against AdipoR1 (ab126611), AdipoR2 (ab77612), UCP1 (ab23841), and C/EBPβ (ab32358) were from Abcam. Anti-LC3B (L7543) from Sigma was used for Western blot, analysis and Anti-LC3 pAb (PM036) from MBL International was used for staining. Anti-adiponectin and anti-β-tubulin were kindly pro-vided by Dr. Lily Dong (University of Texas Health Science Center at San Antonio, San Antonio, TX) as described previously (Alsted et al., 2009; Meng et al., 2017). AdipoRon (924416–43-3) and 5Z (253863–19-3) were obtained from Cayman Chemical Company. IRAK 1/4 inhibitor I (I5409) and rapamycin (R8781) were from Sigma-Aldrich. 3-MA (189490) was purchased from EMD Millipore. Two recombinant mouse adiponectin (full-length and mutated C39A) proteins (ab62957 and ab94676) were purchased from Abcam. Mouse ST2/IL-1 R4 antibody (MAB10041) was from R&D Systems.

Mice
All mice used in this study were males unless specified other-wise. Adiponectin knockout mice were kindly provided by Dr. Philipp Scherer (University of Texas Southwestern Medical Center, Dallas, TX). This mouse line was crossed with C57BL/6J (stock no. 000664) for >10 generations before the study began. Both Rag2 KO mice (stock no. 008449) and Il2rg KO mice (stock no. 003174) with C57BL/6J background were purchased from Jackson Laboratory. We generated Rag2/Il2rg double-KO mice by crossing the Rag2 KO mice and Il2rg KO mice and then in-breeding the resulting Rag2/Il2rg heterozygous offspring. An-other stain of adiponectin-deficient mouse was ordered from Jackson Laboratory (B6;129-Adipoqtm1Chan/J, stock no. 008195; Adipo-) and backcrossed with C57BL/6 mice for four generations to validate the antithermogenic function of adiponectin. All animals were housed in a pathogen-free barrier facility with a 12-h light/12-h dark cycle with free access to food and water. All animal experimental protocols were reviewed and approved by the Animal Care Committee of the University of New Mexico Health Sciences Center. For cold stress studies, the mice were housed in an environmental chamber at 30°C followed by 48 h of either 22°C or 6°C and then euthanized for Western blot analysis, as described in our previous study (Ding et al., 2016; Wang et al., 2018).

Isolation and treatment of adipose tissue ILC2s
SVFs were isolated from subcutaneous and epididymal white fat of 2–3-mo-old male mice and then blocked with fragment crystallizable region-block (homemade) at 4°C for 20 min. For the signaling study of ILC2s, F4/80$^+$, Gr-1$^+$, and CD3$^+$ cells were depleted using the indicated antibodies and magnetic beads. Cells were then incubated with ST2 antibody, and ST2$^+$ cells were pulled down by loading the tube onto the magnetic rack (Invitrogen) for 5 min. Cell pellets were suspended in medium containing RPMI 1640 and 1% FBS for the following treatment. For the signaling study, there were the following three types of treatment: (1) cells were treated with 10 ng/ml IL-33 only for 10 min; (2) cells were treated with 10 µM AdipoRon or 5 µg/ml full-length adiponectin for 1 h, followed by cotreatment with IL-33 for 10 min; and (3) cells were treated with 1 µM AMPK in-hibitor compound C for 20 min, followed with cotreatment with IL-33 for 20 min. The phosphorylation of IKKα/β, IκBα, or AMPK was determined using flow cytometry with specific antibodies. For the ELISA analysis, fragment crystallizable region-blocked SVF cells were washed and stained with anti-CD45-PE, anti-Lin (CD11b, CD11c, B220, CD3, Gr-1)-PerCP, anti-ST2-APC for 20 min on ice. Then, live CD45$^+$Lin$^-$ST2$^+$ ILC2s were sort-purified by a Sony iCyt SY3200 four-laser cell sorter to 95% purity, and 10^5 cells were harvested in TriZol buffer. For the measurement of IL-13 secretion, ILC2s or SVFs were cultured in the medium containing 10% FBS and treated with 5 µg/ml full-length adi-ponectin or 1 µM compound C for 1 h followed by cotreatment with IL-33 for 18 h, and media was collected for ELISA analysis.

Primary culture and differentiation of Th2 cells
CD45R$^-$CD8a$^-$CD62L$^+$ naive T cells were isolated from lymph nodes and spleens in 2–3-mo-old C57BL/6 WT mice using beads.

Cells were then seeded on a plate coated with α-CD3/α-CD28 and differentiated into Th2 cells using a RPMI medium containing 10% FBS, 5 μg/ml anti-IFNγ, and 10 ng/ml IL-4 for 72 h. To suppress TAK1 and AMPK in differentiated Th2 cells, siRNA of TAK1 or siRNA of AMPKα1/2 and the control siRNA were introduced into Th2 cells using electroporation with Neon transfection system (1,600 V, 10 mS/pulse, three pulses). 30 h after transfection, TAK1-suppressed and scramble cells were cultured in a fresh RPMI medium with 1% FBS for 1 h and then treated with or without 10 ng/ml IL-33 for 10 min. To determine the role of AMPK in regulating IL-33 signaling, AMPK-suppressed and scramble cells were cultured in a fresh RPMI medium with 1% FBS for 1 h and then treated with (1) 10 ng/ml IL-33 only for 10 min; (2) 10 μM AdipoRon or 5 μg/ml full-length adiponectin for 1 h, followed by cotreatment with IL-33 for 10 min; or (3) 1 μM AMPK inhibitor compound C for 20 min, followed by cotreatment with IL-33 for 20 min. In addition, starved Th2 cells were treated with 10 ng/ml IL-33 only for 10 min, 10 μM AdipoRon, or 5 μg/ml full-length adiponectin for 1 h, followed by cotreatment with IL-33 for 10 min or 1 μM AMPK inhibitor compound C for 20 min and cotreatment with IL-33 for 20 min.

ELISA analysis of IL-13 and IL-4
For the measurement of IL-13 and IL-4 secretion, SVFs from adipose tissue were cultured in FBS-free medium containing 0.5% BSA and then treated with or without 5 μg/ml full-length adiponectin for 1 h followed by treatment with or without 10 ng/ml IL-33 for 18 h. The media was collected for ELISA analysis of IL-13 and IL-4. The ELISA assay for IL-13 or IL-4 from ILC2s and/or SVFs was determined using an ELISA kit (R&D Systems) according to the manufacturer's protocol.

Proliferation and cell death assay of ILC2s
For the proliferation assay, epididymal fat samples from 7-wk-old adiponectin WT and KO mice were dissected, minced, digested with collagenase A (Roche), and filtered with 70 μm cell strainer (Falcon). The SVF were isolated and fixed with 4% polyformaldehyde at 4°C for 15 min. Ki67 expression in ILC2s was measured by intracellular staining on a CD45+Lin−ST2+gate. Lin (lineage marker) included CD3, B220, CD11b, CD11c, and Gr-1. For the cell death assay, the underlying pellets (SVF) and media remained. ILC2s were assessed by LIVE/DEAD Green (LIVE/DEAD Fixable Dead Cell Stain Kit; Invitrogen) reactive to free amines both in the interior and on the cell surface as we described previously (Zheng et al., 2018).

Adiponectin or AdipoRon administration
For i.p. administration, AdipoRon was dissolved in DMSO and diluted by vehicle solution, which contained 5% Tween 80 and 5% polyethylene glycol 400 in PBS. 10-wk-old adiponectin KO male mice were administered with AdipoRon or vehicle by i.p. injection at 30 mg/kg body weight once a day for 5 d. 24 h after the first administration, the calorimetry study was performed. The mice were euthanized after 48 h of cold conditions, and fat tissues were harvested for Western blot analysis. For i.c.v. administration, 10-wk-old mice underwent cannula implantation surgery and recovered for 2 wk. 2 μl trimeric (C39A)

adiponectin (1 mg/ml) or vehicle was pumped into cerebral ventricle by micro syringe pump at the speed of 1 μl/minute. For the intra-iWAT administration, the procedure was performed on 10-wk-old mice as described in the previous study (Murphy et al., 2013). In brief, AdipoRon or vehicle (3 mg/kg body mass) was administered at five sites across the inguinal white adipose depot by a syringe equipped with a 30-gauge needle. Calorimetry studies were performed at 6°C, after i.c.v. or intra-iWAT injection, and fat tissues were harvested for Western blot analysis.

Administration of IL-33 receptor antibody
10-wk-old male adiponectin WT and KO mice were administered with or without mouse ST2/IL-1 R4 antibody (R&D Systems) at 100 μg/mice/day by i.p. injection under cold exposure (6°C) for 2 d. The mice were euthanized, and adipose tissues were collected for flow cytometry analysis and Western blot analysis.

Flow cytometry
The suspended SVFs from adipose depots of 10-wk-old male mice were fixed, blocked, and stained with conjugated antibodies, including anti-CD45, anti-Siglec-5, anti-CD11b, and anti-CD206 (eBioscience and BioLegend), to identify macrophage subsets. To detect ILC2s (CD45+Lin−CD90.2+ST2+), SVF cells were incubated with conjugated anti-CD45, anti-Lin (CD3e, CD11b, B220, CD11c, and Gr-1), anti-CD90.2, and anti-ST2 (eBioscience and BioLegend) after fixation unless specified otherwise. In Fig. S1 D, we used additional markers, including anti-RORC and anti-GATA3 (eBioscience), to gate ILC2s (CD45+Lin−CD90.2+RORC−ST2+GATA3+). Anti-AMPK α 1 (phospho-T183) and AMPK α 2 (phospho-T172) antibody (ab23875; Abcam), eFluor 660–conjugated anti-phospho-IκBα (S32/S36; eBioscience), and PE-conjugated phospho-IKKα/β (Ser176/180; Cell Signaling) were used to detect phospho-AMPK, phospho-IκBα and phospho-IKK in ILC2. For the staining of GATA3, RORC and phosphorylated proteins, cells were permeabilized with 0.25% Triton X-100 for 20 min after fixation. FACS analysis was performed on a FACS Calibur (BD PharMingen), and the data were analyzed with FlowJo software as described previously (Dong et al., 2013). The gating strategy used for ILC2s, eosinophils, and macrophages in adipose tissue is shown in Fig. S3, I–K.

Energy expenditure
10-wk-old male mice were individually housed in eight separate Promethion Metabolic Phenotyping Systems (Sable Systems International) coupled with a temperature controllable chamber. O_2 consumption, carbon dioxide release, food intake, water intake, and the activity of each animal were monitored at room temperature (22°C) for 72 h and then in cold stress conditions (6°C) for 48 h. The data were analyzed using the ExpeData software associated with the system. O_2 consumption was normalized by body weight as we described previously (Luo et al., 2017; Zhang et al., 2018).

Telemetry study
The Mini-Mitter Telemetry System was used for the measurement of core body temperature in adiponectin KO and WT mice

as we described previously (Liu et al., 2014). Briefly, a Mini-Mitter implantable biotelemetric thermosensor was surgically implanted into the peritoneal cavity of 10-wk-old male mice. 10 d after surgery, mice were individually housed in the cage with free access to food and water at room temperature (22°C) for 12 h (8 a.m. to 8 p.m.) followed by exposure to cold stress (6°C) for 12 h (8 p.m. to 8 a.m.). The body temperature and locomotor activity were recorded every 5 min and analyzed with VitalView software.

Western blot

For tissue samples, frozen samples of BAT were sliced and ~1 mg tissue sample was homogenized for Western blot analysis. For the iWAT samples, tissue samples around the lymph node in the inguinal fat was used for the Western blot considering that UCP1+ cells are predominantly in the inguinal region rather than the dorsolumbar region after a 2-d cold exposure within a posterior subcutaneous fat pad (Chi et al., 2018). Cell lysates were prepared in ice-cold lysis buffer, and the general procedures were used for Western blot as described in our previous study (Liu et al., 2008). For all Western blot data presented in this study, the x axis indicates the individual mouse or the individual cell treatment.

Induction of allergic asthma

For induction of allergic asthma, age-matched adiponectin KO and WT male littermates were immunized intranasally with 15 µg papain and 50 µg chicken OVA for three times on days 0, 1, and 14 as we described previously (Zheng et al., 2016). 14 d after the first-time immunization with papain and OVA, bronchoalveolar lavage fluids (BALFs) were collected for analysis of airway infiltrates. Lung-draining LNs (LLNs) were collected for cytokine expression and proliferation assays. LLN cells (4×10^6 cells/ml) from the asthmatic mice were cultured with various concentrations of OVA for 3 d, and the supernatants were collected for measurement of cytokine expression by ELISA using a standard protocol. For the in vivo proliferation assay, single-cell suspensions of LLNs from asthmatic mice were prepared, and Ki67 expression was measured in Th2 cells (Lin+CD4+GATA3+), ILC2s (Lin−CD4−GATA3+), and Th1 cells (Lin+CD4+IFNγ+). Lineage markers include CD3, CD5, B220, CD11b, CD11c, Gr-1, Ter119, and IgE. Antibodies to CD3, CD5, B220, CD11b, CD11c, Gr-1, Ter119, IgE, CD4, GATA3, IFNγ, and Ki67 were purchased from eBioscience.

Statistics

Effects of various treatments on the expression levels of norepinephrine and UCP1 in cells were analyzed by t test for comparison of two groups or one-way ANOVA for comparison of more than two groups. ANOVA was used for the statistical analysis of energy expenditure. For each group, 5–10 animals were used for in vivo experiments. The individual in vitro experiment was repeated at least three times. Data are presented as means ± SEM. $P < 0.05$ was considered as significant.

Online supplemental material

Fig. S1 shows that adiponectin deficiency promotes a type 2 immune response in adipose tissue and allergic airway. Fig. S2 indicates that adiponectin inhibits thermogenesis in a peripheral tissue–dependent manner. Fig. S3 demonstrates that adiponectin

KO also increases O_2 consumption and up-regulates thermogenic gene expression and ILC2 activation in adipose tissue of another mouse model and describes the gating strategy used for flow cytometric analysis in adipose tissue.

References

Abbasi, F., J.W. Chu, C. Lamendola, T. McLaughlin, J. Hayden, G.M. Reaven, and P.D. Reaven. 2004. Discrimination between obesity and insulin resistance in the relationship with adiponectin. *Diabetes.* 53:585–590. https://doi.org/10.2337/diabetes.53.3.585

Ahima, R.S. 2006. Metabolic actions of adipocyte hormones: focus on adiponectin. *Obesity (Silver Spring).* 14(2S, Suppl 1):9S–15S. https://doi.org/10.1038/oby.2006.276

Ajuwon, K.M., and M.E. Spurlock. 2005. Adiponectin inhibits LPS-induced NF-kappaB activation and IL-6 production and increases PPARgamma2 expression in adipocytes. *Am. J. Physiol. Regul. Integr. Comp. Physiol.* 288: R1220–R1225. https://doi.org/10.1152/ajpregu.00397.2004

Ali, S., A. Mohs, M. Thomas, J. Klare, R. Ross, M.L. Schmitz, and M.U. Martin. 2011. The dual function cytokine IL-33 interacts with the transcription factor NF-κB to dampen NF-κB-stimulated gene transcription. *J. Immunol.* 187:1609–1616. https://doi.org/10.4049/jimmunol.1003080

Alsted, T.J., L. Nybo, M. Schweiger, C. Fledelius, P. Jacobsen, R. Zimmermann, R. Zechner, and B. Kiens. 2009. Adipose triglyceride lipase in human skeletal muscle is upregulated by exercise training. *Am. J. Physiol. Endocrinol. Metab.* 296:E445–E453. https://doi.org/10.1152/ajpendo.90912.2008

Antonia, R.J., and A.S. Baldwin. 2018. IKK promotes cytokine-induced and cancer-associated AMPK activity and attenuates phenformin-induced cell death in LKB1-deficient cells. *Sci. Signal.* 11:eaan5850. https://doi.org/10.1126/scisignal.aan5850

Awazawa, M., K. Ueki, K. Inabe, T. Yamauchi, N. Kubota, K. Kaneko, M. Kobayashi, A. Iwane, T. Sasako, Y. Okazaki, et al. 2011. Adiponectin enhances insulin sensitivity by increasing hepatic IRS-2 expression via a macrophage-derived IL-6-dependent pathway. *Cell Metab.* 13:401–412. https://doi.org/10.1016/j.cmet.2011.02.010

Bauche, I.B., S.A. El Mkadem, A.M. Pottier, M. Senou, M.C. Many, R. Rezsohazy, L. Penicaud, N. Maeda, T. Funahashi, and S.M. Brichard. 2007. Overexpression of adiponectin targeted to adipose tissue in transgenic mice: impaired adipocyte differentiation. *Endocrinology.* 148:1539–1549. https://doi.org/10.1210/en.2006-0838

Blagih, J., F. Coulombe, E.E. Vincent, F. Dupuy, G. Galicia-Vázquez, E. Yurchenko, T.C. Raissi, G.J. van der Windt, B. Viollet, E.L. Pearce, et al. 2015. The energy sensor AMPK regulates T cell metabolic adaptation and effector responses in vivo. *Immunity.* 42:41–54. https://doi.org/10.1016/j.immuni.2014.12.030

Boström, P., J. Wu, M.P. Jedrychowski, A. Korde, L. Ye, J.C. Lo, K.A. Rasbach, E.A. Boström, J.H. Choi, J.Z. Long, et al. 2012. A PGC1-α-dependent myokine that drives brown-fat-like development of white fat and thermogenesis. *Nature.* 481:463–468. https://doi.org/10.1038/nature10777

Brestoff, J.R., B.S. Kim, S.A. Saenz, R.R. Stine, L.A. Monticelli, G.F. Sonnenberg, J.J. Thome, D.L. Farber, K. Lutfy, P. Seale, and D. Artis. 2015. Group 2 innate lymphoid cells promote beiging of white adipose tissue and limit obesity. *Nature.* 519:242–246. https://doi.org/10.1038/nature14115

Cao, Z., J. Xiong, M. Takeuchi, T. Kurama, and D.V. Goeddel. 1996. TRAF6 is a signal transducer for interleukin-1. *Nature.* 383:443–446. https://doi.org/10.1038/383443a0

Carling, D. 2004. The AMP-activated protein kinase cascade--a unifying system for energy control. *Trends Biochem. Sci.* 29:18–24. https://doi.org/10.1016/j.tibs.2003.11.005

Cayrol, C., and J.P. Girard. 2014. IL-33: an alarmin cytokine with crucial roles in innate immunity, inflammation and allergy. *Curr. Opin. Immunol.* 31: 31–37. https://doi.org/10.1016/j.coi.2014.09.004

Chen, Z., X. Shen, F. Shen, W. Zhong, H. Wu, S. Liu, and J. Lai. 2013. TAK1 activates AMPK-dependent cell death pathway in hydrogen peroxide-treated cardiomyocytes, inhibited by heat shock protein-70. *Mol. Cell. Biochem.* 377:35–44. https://doi.org/10.1007/s11010-013-1568-z

Cheng, X., E.J. Folco, K. Shimizu, and P. Libby. 2012. Adiponectin induces pro-inflammatory programs in human macrophages and CD4+ T cells. *J. Biol. Chem.* 287:36896–36904. https://doi.org/10.1074/jbc.M112.409516

Chi, J., Z. Wu, C.H.J. Choi, L. Nguyen, S. Tegegne, S.E. Ackerman, A. Crane, F. Marchildon, M. Tessier-Lavigne, and P. Cohen. 2018. Three-Dimensional Adipose Tissue Imaging Reveals Regional Variation in Beige Fat Biogenesis and PRDM16-Dependent Sympathetic Neurite Density. *Cell Metab.* 27:226–236.e3. https://doi.org/10.1016/j.cmet.2017.12.011

Coleman, D.L., and K.P. Hummel. 1973. The influence of genetic background on the expression of the obese (Ob) gene in the mouse. *Diabetologia.* 9: 287–293. https://doi.org/10.1007/BF01221856

Ding, X., Y. Luo, X. Zhang, H. Zheng, X. Yang, X. Yang, and M. Liu. 2016. IL-33-driven ILC2/eosinophil axis in fat is induced by sympathetic tone and suppressed by obesity. *J. Endocrinol.* 231:35–48. https://doi.org/10.1530/JOE-16-0229

Dong, M., X. Yang, S. Lim, Z. Cao, J. Honek, H. Lu, C. Zhang, T. Seki, K. Hosaka, E. Wahlberg, et al. 2013. Cold exposure promotes atherosclerotic plaque growth and instability via UCP1-dependent lipolysis. *Cell Metab.* 18:118–129. https://doi.org/10.1016/j.cmet.2013.06.003

Duran, A., J.F. Linares, A.S. Galvez, K. Wikenheiser, J.M. Flores, M.T. Diaz-Meco, and J. Moscat. 2008. The signaling adaptor p62 is an important NF-kappaB mediator in tumorigenesis. *Cancer Cell.* 13:343–354. https://doi.org/10.1016/j.ccr.2008.02.001

Fischer, K., H.H. Ruiz, K. Jhun, B. Finan, D.J. Oberlin, V. van der Heide, A.V. Kalinovich, N. Petrovic, Y. Wolf, C. Clemmensen, et al. 2017. Alternatively activated macrophages do not synthesize catecholamines or contribute to adipose tissue adaptive thermogenesis. *Nat. Med.* 23: 623–630. https://doi.org/10.1038/nm.4316

Fisher, F.M., S. Kleiner, N. Douris, E.C. Fox, R.J. Mepani, F. Verdeguer, J. Wu, A. Kharitonenkov, J.S. Flier, E. Maratos-Flier, and B.M. Spiegelman. 2012. FGF21 regulates PGC-1α and browning of white adipose tissues in adaptive thermogenesis. *Genes Dev.* 26:271–281. https://doi.org/10.1101/gad.177857.111

Fontaine, D.A., and D.B. Davis. 2016. Attention to Background Strain Is Essential for Metabolic Research: C57BL/6 and the International Knockout Mouse Consortium. *Diabetes.* 65:25–33. https://doi.org/10.2337/db15-0982

Guo, L., I.S. Junttila, and W.E. Paul. 2012. Cytokine-induced cytokine production by conventional and innate lymphoid cells. *Trends Immunol.* 33: 598–606. https://doi.org/10.1016/j.it.2012.07.006

Hardie, D.G. 2004. The AMP-activated protein kinase pathway--new players upstream and downstream. *J. Cell Sci.* 117:5479–5487. https://doi.org/10.1242/jcs.01540

Hawley, S.A., D.A. Pan, K.J. Mustard, L. Ross, J. Bain, A.M. Edelman, B.G. Frenguelli, and D.G. Hardie. 2005. Calmodulin-dependent protein kinase kinase-beta is an alternative upstream kinase for AMP-activated protein kinase. *Cell Metab.* 2:9–19. https://doi.org/10.1016/j.cmet.2005.05.009

Herrero-Martín, G., M. Høyer-Hansen, C. García-García, C. Fumarola, T. Farkas, A. López-Rivas, and M. Jäättelä. 2009. TAK1 activates AMPK-dependent cytoprotective autophagy in TRAIL-treated epithelial cells. *EMBO J.* 28:677–685. https://doi.org/10.1038/emboj.2009.8

Holland, W.L., A.C. Adams, J.T. Brozinick, H.H. Bui, Y. Miyauchi, C.M. Kusminski, S.M. Bauer, M. Wade, E. Singhal, C.C. Cheng, et al. 2013. An FGF21-adiponectin-ceramide axis controls energy expenditure and insulin action in mice. *Cell Metab.* 17:790–797. https://doi.org/10.1016/j.cmet.2013.03.019

Hui, X., P. Gu, J. Zhang, T. Nie, Y. Pan, D. Wu, T. Feng, C. Zhong, Y. Wang, K.S. Lam, and A. Xu. 2015. Adiponectin Enhances Cold-Induced Browning of Subcutaneous Adipose Tissue via Promoting M2 Macrophage Proliferation. *Cell Metab.* 22:279–290. https://doi.org/10.1016/j.cmet.2015.06.004

Hummel, K.P., D.L. Coleman, and P.W. Lane. 1972. The influence of genetic background on expression of mutations at the diabetes locus in the mouse. I. C57BL-KsJ and C57BL-6J strains. *Biochem. Genet.* 7:1–13. https://doi.org/10.1007/BF00487005

Kadowaki, T., and T. Yamauchi. 2005. Adiponectin and adiponectin receptors. *Endocr. Rev.* 26:439–451. https://doi.org/10.1210/er.2005-0005

Kajimura, D., H.W. Lee, K.J. Riley, E. Arteaga-Solis, M. Ferron, B. Zhou, C.J. Clarke, Y.A. Hannun, R.A. DePinho, X.E. Guo, et al. 2013. Adiponectin regulates bone mass via opposite central and peripheral mechanisms through FoxO1. *Cell Metab.* 17:901–915. https://doi.org/10.1016/j.cmet.2013.04.009

Kim, J.Y., E. van de Wall, M. Laplante, A. Azzara, M.E. Trujillo, S.M. Hofmann, T. Schraw, J.L. Durand, H. Li, G. Li, et al. 2007. Obesity-associated improvements in metabolic profile through expansion of adipose tissue. *J. Clin. Invest.* 117:2621–2637. https://doi.org/10.1172/JCI31021

Kolodin, D., N. van Panhuys, C. Li, A.M. Magnuson, D. Cipolletta, C.M. Miller, A. Wagers, R.N. Germain, C. Benoist, and D. Mathis. 2015. Antigen- and cytokine-driven accumulation of regulatory T cells in visceral adipose tissue of lean mice. *Cell Metab.* 21:543–557. https://doi.org/10.1016/j.cmet.2015.03.005

Koyasu, S., and K. Moro. 2013. Th2-type innate immune responses mediated by natural helper cells. *Ann. N. Y. Acad. Sci.* 1283:43–49. https://doi.org/10.1111/nyas.12106

Kubota, N., W. Yano, T. Kubota, T. Yamauchi, S. Itoh, H. Kumagai, H. Kozono, I. Takamoto, S. Okamoto, T. Shiuchi, et al. 2007. Adiponectin stimulates AMP-activated protein kinase in the hypothalamus and increases food intake. *Cell Metab.* 6:55–68. https://doi.org/10.1016/j.cmet.2007.06.003

Kumada, M., S. Kihara, N. Ouchi, H. Kobayashi, Y. Okamoto, K. Ohashi, K. Maeda, H. Nagaretani, K. Kishida, N. Maeda, et al. 2004. Adiponectin specifically increased tissue inhibitor of metalloproteinase-1 through interleukin-10 expression in human macrophages. *Circulation.* 109: 2046–2049. https://doi.org/10.1161/01.CIR.0000127953.98131.ED

Kuswanto, W., D. Burzyn, M. Panduro, K.K. Wang, Y.C. Jang, A.J. Wagers, C. Benoist, and D. Mathis. 2016. Poor Repair of Skeletal Muscle in Aging

Mice Reflects a Defect in Local, Interleukin-33-Dependent Accumulation of Regulatory T Cells. *Immunity.* 44:355–367. https://doi.org/10.1016/j.immuni.2016.01.009

Lallena, M.J., M.T. Diaz-Meco, G. Bren, C.V. Payá, and J. Moscat. 1999. Activation of IkappaB kinase beta by protein kinase C isoforms. *Mol. Cell. Biol.* 19:2180–2188. https://doi.org/10.1128/MCB.19.3.2180

Lee, M.W., J.I. Odegaard, L. Mukundan, Y. Qiu, A.B. Molofsky, J.C. Nussbaum, K. Yun, R.M. Locksley, and A. Chawla. 2015. Activated type 2 innate lymphoid cells regulate beige fat biogenesis. *Cell.* 160:74–87. https://doi.org/10.1016/j.cell.2014.12.011

Lei, A.H., Q. Xiao, G.Y. Liu, K. Shi, Q. Yang, X. Li, Y.F. Liu, H.K. Wang, W.P. Cai, Y.J. Guan, et al. 2018. ICAM-1 controls development and function of ILC2. *J. Exp. Med.* 215:2157–2174. https://doi.org/10.1084/jem.20172359

Li, Q., D. Li, X. Zhang, Q. Wan, W. Zhang, M. Zheng, L. Zou, C. Elly, J.H. Lee, and Y.C. Liu. 2018. E3 Ligase VHL Promotes Group 2 Innate Lymphoid Cell Maturation and Function via Glycolysis Inhibition and Induction of Interleukin-33 Receptor. *Immunity.* 48:258–270.e5. https://doi.org/10.1016/j.immuni.2017.12.013

Licona-Limón, P., L.K. Kim, N.W. Palm, and R.A. Flavell. 2013. Th2, allergy and group 2 innate lymphoid cells. *Nat. Immunol.* 14:536–542. https://doi.org/10.1038/ni.2617

Liu, M., L. Zhou, A. Xu, K.S. Lam, M.D. Wetzel, R. Xiang, J. Zhang, X. Xin, L.Q. Dong, and F. Liu. 2008. A disulfide-bond A oxidoreductase-like protein (DsbA-L) regulates adiponectin multimerization. *Proc. Natl. Acad. Sci. USA.* 105:18302–18307. https://doi.org/10.1073/pnas.0806341105

Liu, M., J. Bai, S. He, R. Villarreal, D. Hu, C. Zhang, X. Yang, H. Liang, T.J. Slaga, Y. Yu, et al. 2014. Grb10 promotes lipolysis and thermogenesis by phosphorylation-dependent feedback inhibition of mTORC1. *Cell Metab.* 19:967–980. https://doi.org/10.1016/j.cmet.2014.03.018

Liu, W., Y. Jiang, J. Sun, S. Geng, Z. Pan, R.A. Prinz, C. Wang, J. Sun, X. Jiao, and X. Xu. 2018. Activation of TGF-β-activated kinase 1 (TAK1) restricts Salmonella Typhimurium growth by inducing AMPK activation and autophagy. *Cell Death Dis.* 9:570. https://doi.org/10.1038/s41419-018-0612-z

Lloyd, C.M. 2010. IL-33 family members and asthma - bridging innate and adaptive immune responses. *Curr. Opin. Immunol.* 22:800–806. https://doi.org/10.1016/j.coi.2010.10.006

Long, Y.C., and J.R. Zierath. 2006. AMP-activated protein kinase signaling in metabolic regulation. *J. Clin. Invest.* 116:1776–1783. https://doi.org/10.1172/JCI29044

Luo, Y., B. Liu, X. Yang, X. Ma, X. Zhang, D.E. Bragin, X.O. Yang, W. Huang, and M. Liu. 2017. Myeloid adrenergic signaling via CaMKII forms a feedforward loop of catecholamine biosynthesis. *J. Mol. Cell Biol.* 9: 422–434. https://doi.org/10.1093/jmcb/mjx046

Ma, K., A. Cabrero, P.K. Saha, H. Kojima, L. Li, B.H. Chang, A. Paul, and L. Chan. 2002. Increased beta -oxidation but no insulin resistance or glucose intolerance in mice lacking adiponectin. *J. Biol. Chem.* 277: 34658–34661. https://doi.org/10.1074/jbc.C200362200

Maeda, N., I. Shimomura, K. Kishida, H. Nishizawa, M. Matsuda, H. Nagaretani, N. Furuyama, H. Kondo, M. Takahashi, Y. Arita, et al. 2002. Diet-induced insulin resistance in mice lacking adiponectin/ACRP30. *Nat. Med.* 8:731–737. https://doi.org/10.1038/nm724

Mao, H.Z., E.T. Roussos, and M. Péterfy. 2006a. Genetic analysis of the diabetes-prone C57BLKS/J mouse strain reveals genetic contribution from multiple strains. *Biochim. Biophys. Acta.* 1762:440–446. https://doi.org/10.1016/j.bbadis.2006.01.002

Mao, X., C.K. Kikani, R.A. Riojas, P. Langlais, L. Wang, F.J. Ramos, Q. Fang, C.Y. Christ-Roberts, J.Y. Hong, R.Y. Kim, et al. 2006b. APPL1 binds to adiponectin receptors and mediates adiponectin signalling and function. *Nat. Cell Biol.* 8:516–523. https://doi.org/10.1038/ncb1404

Martin, P., M.T. Diaz-Meco, and J. Moscat. 2006. The signaling adapter p62 is an important mediator of T helper 2 cell function and allergic airway inflammation. *EMBO J.* 25:3524–3533. https://doi.org/10.1038/sj.emboj.7601250

Masaki, T., S. Chiba, T. Yasuda, T. Tsubone, T. Kakuma, I. Shimomura, T. Funahashi, Y. Matsuzawa, and H. Yoshimatsu. 2003. Peripheral, but not central, administration of adiponectin reduces visceral adiposity and upregulates the expression of uncoupling protein in agouti yellow (Ay/a) obese mice. *Diabetes.* 52:2266–2273. https://doi.org/10.2337/diabetes.52.9.2266

Meng, W., X. Liang, H. Chen, H. Luo, J. Bai, G. Li, Q. Zhang, T. Xiao, S. He, Y. Zhang, et al. 2017. Rheb Inhibits Beiging of White Adipose Tissue via PDE4D5-Dependent Downregulation of the cAMP-PKA Signaling Pathway. *Diabetes.* 66:1198–1213. https://doi.org/10.2337/db16-0886

Miller, A.M., D.L. Asquith, A.J. Hueber, L.A. Anderson, W.M. Holmes, A.N. McKenzie, D. Xu, N. Sattar, I.B. McInnes, and F.Y. Liew. 2010. Interleukin-33 induces protective effects in adipose tissue inflammation during obesity in mice. *Circ. Res.* 107:650–658. https://doi.org/10.1161/CIRCRESAHA.110.218867

Molofsky, A.B., J.C. Nussbaum, H.E. Liang, S.J. Van Dyken, L.E. Cheng, A. Mohapatra, A. Chawla, and R.M. Locksley. 2013. Innate lymphoid type 2 cells sustain visceral adipose tissue eosinophils and alternatively activated macrophages. *J. Exp. Med.* 210:535–549. https://doi.org/10.1084/jem.20121964

Molofsky, A.B., F. Van Gool, H.E. Liang, S.J. Van Dyken, J.C. Nussbaum, J. Lee, J.A. Bluestone, and R.M. Locksley. 2015. Interleukin-33 and Interferon-γ Counter-Regulate Group 2 Innate Lymphoid Cell Activation during Immune Perturbation. *Immunity.* 43:161–174. https://doi.org/10.1016/j.immuni.2015.05.019

Momcilovic, M., S.P. Hong, and M. Carlson. 2006. Mammalian TAK1 activates Snf1 protein kinase in yeast and phosphorylates AMP-activated protein kinase in vitro. *J. Biol. Chem.* 281:25336–25343. https://doi.org/10.1074/jbc.M604399200

Moro, K., T. Yamada, M. Tanabe, T. Takeuchi, T. Ikawa, H. Kawamoto, J. Furusawa, M. Ohtani, H. Fujii, and S. Koyasu. 2010. Innate production of T(H)2 cytokines by adipose tissue-associated c-Kit(+)Sca-1(+) lymphoid cells. *Nature.* 463:540–544. https://doi.org/10.1038/nature08636

Murphy, K.T., G.J. Schwartz, N.L. Nguyen, J.M. Mendez, V. Ryu, and T.J. Bartness. 2013. Leptin-sensitive sensory nerves innervate white fat. *Am. J. Physiol. Endocrinol. Metab.* 304:E1338–E1347. https://doi.org/10.1152/ajpendo.00021.2013

Nawrocki, A.R., M.W. Rajala, E. Tomas, U.B. Pajvani, A.K. Saha, M.E. Trumbauer, Z. Pang, A.S. Chen, N.B. Ruderman, H. Chen, et al. 2006. Mice lacking adiponectin show decreased hepatic insulin sensitivity and reduced responsiveness to peroxisome proliferator-activated receptor gamma agonists. *J. Biol. Chem.* 281:2654–2660. https://doi.org/10.1074/jbc.M505311200

Newland, S.A., S. Mohanta, M. Clément, S. Taleb, J.A. Walker, M. Nus, A.P. Sage, C. Yin, D. Hu, L.L. Kitt, et al. 2017. Type-2 innate lymphoid cells control the development of atherosclerosis in mice. *Nat. Commun.* 8: 15781. https://doi.org/10.1038/ncomms15781

Odegaard, J.I., M.W. Lee, Y. Sogawa, A.M. Bertholet, R.M. Locksley, D.E. Weinberg, Y. Kirichok, R.C. Deo, and A. Chawla. 2016. Perinatal Licensing of Thermogenesis by IL-33 and ST2. *Cell.* 166:841–854. https://doi.org/10.1016/j.cell.2016.06.040

Ohashi, K., J.L. Parker, N. Ouchi, A. Higuchi, J.A. Vita, N. Gokce, A.A. Pedersen, C. Kalthoff, S. Tullin, A. Sams, et al. 2010. Adiponectin promotes macrophage polarization toward an anti-inflammatory phenotype. *J. Biol. Chem.* 285:6153–6160. https://doi.org/10.1074/jbc.M109.088708

Okada-Iwabu, M., T. Yamauchi, M. Iwabu, T. Honma, K. Hamagami, K. Matsuda, M. Yamaguchi, H. Tanabe, T. Kimura-Someya, M. Shirouzu, et al. 2013. A small-molecule AdipoR agonist for type 2 diabetes and short life in obesity. *Nature.* 503:493–499. https://doi.org/10.1038/nature12656

Oldenhove, G., E. Boucquey, A. Taquin, V. Acolty, L. Bonetti, B. Ryffel, M. Le Bert, K. Englebert, L. Boon, and M. Moser. 2018. PD-1 Is Involved in the Dysregulation of Type 2 Innate Lymphoid Cells in a Murine Model of Obesity. *Cell Rep.* 25:2053–2060.e4. https://doi.org/10.1016/j.celrep.2018.10.091

Park, P.H., M.R. McMullen, H. Huang, V. Thakur, and L.E. Nagy. 2007. Short-term treatment of RAW264.7 macrophages with adiponectin increases tumor necrosis factor-alpha (TNF-alpha) expression via ERK1/2 activation and Egr-1 expression: role of TNF-alpha in adiponectin-stimulated interleukin-10 production. *J. Biol. Chem.* 282:21695–21703. https://doi.org/10.1074/jbc.M701419200

Petrovic, N., T.B. Walden, I.G. Shabalina, J.A. Timmons, B. Cannon, and J. Nedergaard. 2010. Chronic peroxisome proliferator-activated receptor gamma (PPARgamma) activation of epididymally derived white adipocyte cultures reveals a population of thermogenically competent, UCP1-containing adipocytes molecularly distinct from classic brown adipocytes. *J. Biol. Chem.* 285:7153–7164. https://doi.org/10.1074/jbc.M109.053942

Qi, Y., N. Takahashi, S.M. Hileman, H.R. Patel, A.H. Berg, U.B. Pajvani, P.E. Scherer, and R.S. Ahima. 2004. Adiponectin acts in the brain to decrease body weight. *Nat. Med.* 10:524–529. https://doi.org/10.1038/nm1029

Qiao, L., H. Yoo, C. Bosco, B. Lee, G.S. Feng, J. Schaack, N.W. Chi, and J. Shao. 2014. Adiponectin reduces thermogenesis by inhibiting brown adipose tissue activation in mice. *Diabetologia.* 57:1027–1036. https://doi.org/10.1007/s00125-014-3180-5

Qiu, Y., K.D. Nguyen, J.I. Odegaard, X. Cui, X. Tian, R.M. Locksley, R.D. Palmiter, and A. Chawla. 2014. Eosinophils and type 2 cytokine signaling in macrophages orchestrate development of functional beige fat. *Cell.* 157:1292–1308. https://doi.org/10.1016/j.cell.2014.03.066

Quaresma, P.G., N. Reencober, T.M. Zanotto, A.C. Santos, L. Weissmann, A.H. de Matos, I. Lopes-Cendes, F. Folli, M.J. Saad, and P.O. Prada. 2016. Pioglitazone treatment increases food intake and decreases energy expenditure partially via hypothalamic adiponectin/adipoR1/AMPK pathway. *Int. J. Obes.* 40:138–146. https://doi.org/10.1038/ijo.2015.134

Rao, R.R., J.Z. Long, J.P. White, K.J. Svensson, J. Lou, I. Lokurkar, M.P. Jedrychowski, J.L. Ruas, C.D. Wrann, J.C. Lo, et al. 2014. Meteorin-like is a hormone that regulates immune-adipose interactions to increase beige fat thermogenesis. *Cell.* 157:1279–1291. https://doi.org/10.1016/j.cell.2014.03.065

Ristow, M., D. Müller-Wieland, A. Pfeiffer, W. Krone, and C.R. Kahn. 1998. Obesity associated with a mutation in a genetic regulator of adipocyte differentiation. *N. Engl. J. Med.* 339:953–959. https://doi.org/10.1056/NEJM199810013391403

Ruan, H., and L.Q. Dong. 2016. Adiponectin signaling and function in insulin target tissues. *J. Mol. Cell Biol.* 8:101–109. https://doi.org/10.1093/jmcb/mjw014

Saito, K., S. Arata, T. Hosono, Y. Sano, K. Takahashi, N.H. Choi-Miura, Y. Nakano, T. Tobe, and M. Tomita. 2006. Adiponectin plays an important role in efficient energy usage under energy shortage. *Biochim. Biophys. Acta.* 1761:709–716. https://doi.org/10.1016/j.bbalip.2006.04.016

Savage, D.B., G.D. Tan, C.L. Acerini, S.A. Jebb, M. Agostini, M. Gurnell, R.L. Williams, A.M. Umpleby, E.L. Thomas, J.D. Bell, et al. 2003. Human metabolic syndrome resulting from dominant-negative mutations in the nuclear receptor peroxisome proliferator-activated receptor-gamma. *Diabetes.* 52:910–917. https://doi.org/10.2337/diabetes.52.4.910

Scherer, P.E. 2006. Adipose tissue: from lipid storage compartment to endocrine organ. *Diabetes.* 55:1537–1545. https://doi.org/10.2337/db06-0263

Scherer, P.E., S. Williams, M. Fogliano, G. Baldini, and H.F. Lodish. 1995. A novel serum protein similar to C1q, produced exclusively in adipocytes. *J. Biol. Chem.* 270:26746–26749. https://doi.org/10.1074/jbc.270.45.26746

Takaesu, G., S. Kishida, A. Hiyama, K. Yamaguchi, H. Shibuya, K. Irie, J. Ninomiya-Tsuji, and K. Matsumoto. 2000. TAB2, a novel adaptor protein, mediates activation of TAK1 MAPKKK by linking TAK1 to TRAF6 in the IL-1 signal transduction pathway. *Mol. Cell.* 5:649–658. https://doi.org/10.1016/S1097-2765(00)80244-0

Tang, C.H., Y.C. Chiu, T.W. Tan, R.S. Yang, and W.M. Fu. 2007. Adiponectin enhances IL-6 production in human synovial fibroblast via an AdipoR1 receptor, AMPK, p38, and NF-kappa B pathway. *J. Immunol.* 179:5483–5492. https://doi.org/10.4049/jimmunol.179.8.5483

Tsao, T.S., H.E. Murrey, C. Hug, D.H. Lee, and H.F. Lodish. 2002. Oligomerization state-dependent activation of NF-kappa B signaling pathway by adipocyte complement-related protein of 30 kDa (Acrp30). *J. Biol. Chem.* 277:29359–29362. https://doi.org/10.1074/jbc.C200312200

Vasanthakumar, A., K. Moro, A. Xin, Y. Liao, R. Gloury, S. Kawamoto, S. Fagarasan, L.A. Mielke, S. Afshar-Sterle, S.L. Masters, et al. 2015. The transcriptional regulators IRF4, BATF and IL-33 orchestrate development and maintenance of adipose tissue-resident regulatory T cells. *Nat. Immunol.* 16:276–285. https://doi.org/10.1038/ni.3085

Wang, C., L. Deng, M. Hong, G.R. Akkaraju, J. Inoue, and Z.J. Chen. 2001. TAK1 is a ubiquitin-dependent kinase of MKK and IKK. *Nature.* 412:346–351. https://doi.org/10.1038/35085597

Wang, Y., J. Chu, P. Yi, W. Dong, J. Saultz, Y. Wang, H. Wang, S. Scoville, J. Zhang, L.C. Wu, et al. 2018. SMAD4 promotes TGF-β-independent NK cell homeostasis and maturation and antitumor immunity. *J. Clin. Invest.* 128:5123–5136. https://doi.org/10.1172/JCI121227

Woods, A., K. Dickerson, R. Heath, S.P. Hong, M. Momcilovic, S.R. Johnstone, M. Carlson, and D. Carling. 2005. Ca2+/calmodulin-dependent protein kinase kinase-beta acts upstream of AMP-activated protein kinase in mammalian cells. *Cell Metab.* 2:21–33. https://doi.org/10.1016/j.cmet.2005.06.005

Wooten, M.W., T. Geetha, M.L. Seibenhener, J.R. Babu, M.T. Diaz-Meco, and J. Moscat. 2005. The p62 scaffold regulates nerve growth factor-induced NF-kappaB activation by influencing TRAF6 polyubiquitination. *J. Biol. Chem.* 280:35625–35629. https://doi.org/10.1074/jbc.C500237200

Wu, X., H. Motoshima, K. Mahadev, T.J. Stalker, R. Scalia, and B.J. Goldstein. 2003. Involvement of AMP-activated protein kinase in glucose uptake stimulated by the globular domain of adiponectin in primary rat adipocytes. *Diabetes.* 52:1355–1363. https://doi.org/10.2337/diabetes.52.6.1355

Xie, M., D. Zhang, J.R. Dyck, Y. Li, H. Zhang, M. Morishima, D.L. Mann, G.E. Taffet, A. Baldini, D.S. Khoury, and M.D. Schneider. 2006. A pivotal role for endogenous TGF-beta-activated kinase-1 in the LKB1/AMP-activated protein kinase energy-sensor pathway. *Proc. Natl. Acad. Sci. USA.* 103:17378–17383. https://doi.org/10.1073/pnas.0604708103

Xu, A., Y. Wang, H. Keshaw, L.Y. Xu, K.S. Lam, and G.J. Cooper. 2003. The fat-derived hormone adiponectin alleviates alcoholic and nonalcoholic fatty liver diseases in mice. *J. Clin. Invest.* 112:91–100. https://doi.org/10.1172/JCI200317797

Yamauchi, T., J. Kamon, Y. Minokoshi, Y. Ito, H. Waki, S. Uchida, S. Yamashita, M. Noda, S. Kita, K. Ueki, et al. 2002. Adiponectin stimulates glucose utilization and fatty-acid oxidation by activating AMP-activated protein kinase. *Nat. Med.* 8:1288–1295. https://doi.org/10.1038/nm788

Zeyda, M., B. Wernly, S. Demyanets, C. Kaun, M. Hämmerle, B. Hantusch, M. Schranz, A. Neuhofer, B.K. Itariu, M. Keck, et al. 2013. Severe obesity increases adipose tissue expression of interleukin-33 and its receptor ST2, both predominantly detectable in endothelial cells of human adipose tissue. *Int. J. Obes.* 37:658–665. https://doi.org/10.1038/ijo.2012.118

Zhang, X., Y. Luo, C. Wang, X. Ding, X. Yang, D. Wu, F. Silva, Z. Yang, Q. Zhou, L. Wang, et al. 2018. Adipose mTORC1 Suppresses Prostaglandin Signaling and Beige Adipogenesis via the CRTC2-COX-2 Pathway. *Cell Rep.* 24:3180–3193. https://doi.org/10.1016/j.celrep.2018.08.055

Zheng, H., X. Zhang, E.F. Castillo, Y. Luo, M. Liu, and X.O. Yang. 2016. Leptin Enhances Th2 and ILC2 Responses in Allergic Airway Disease. *J. Biol. Chem.* 291:22043–22052. https://doi.org/10.1074/jbc.M116.743187

Zheng, H., D. Wu, X. Wu, X. Zhang, Q. Zhou, Y. Luo, X. Yang, C.J. Chock, M. Liu, and X.O. Yang. 2018. Leptin Promotes Allergic Airway Inflammation through Targeting the Unfolded Protein Response Pathway. *Sci. Rep.* 8:8905. https://doi.org/10.1038/s41598-018-27278-4

Zhu, J. 2015. T helper 2 (Th2) cell differentiation, type 2 innate lymphoid cell (ILC2) development and regulation of interleukin-4 (IL-4) and IL-13 production. *Cytokine.* 75:14–24. https://doi.org/10.1016/j.cyto.2015.05.010
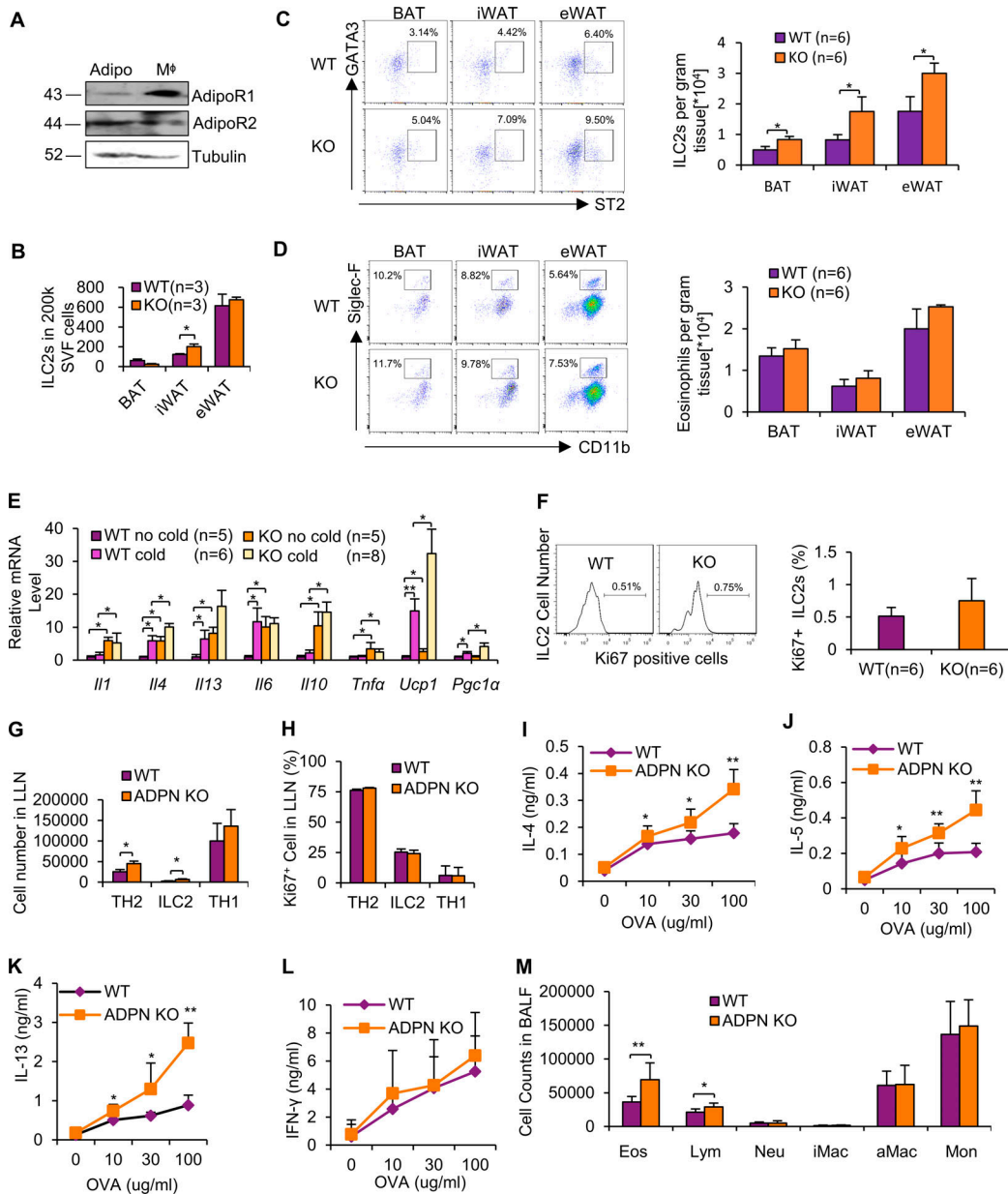
Figure S1.   **Adiponectin deficiency promotes type 2 immune response in adipose tissue and allergic airway. (A)** Adiponectin receptor 1 and 2 (*AdipoR1* and *AdipoR2*) were expressed in differentiated adipocytes (Adipo) and primary macrophages (MΦ). Representative data are presented from two independent experiments. **(B)** Adiponectin deficiency slightly increased the population of ILC2 (CD45⁺Lin⁻CD90.2⁺ST2⁺) in eWAT and iWAT, but not in BAT, at room temperature, while the difference in eWAT did not reach significance. n = 3/group. Data are presented as means ± SEM. *, P < 0.05, Student's t test. **(C)** Adiponectin deficiency significantly increased the population of ILC2 (CD45⁺Lin⁻CD90.2⁺RORC⁻ST2⁺GATA3⁺) in brown (BAT), inguinal (iWAT), and epididymal (eWAT) at 6°C. n = 6/group. Data are presented as means ± SEM, *, P < 0.05, Student's t test. **(D)** Adiponectin deficiency did not change the population of eosinophils (CD11b⁺Siglec-F⁺) in BAT, iWAT, and eWAT. n = 6/group. Data are presented as means ± SEM, *, P < 0.05, Student's t test. **(E)** Adiponectin deficiency up-regulated mRNA levels of thermogenic markers UCP1 and type 2 cytokines such as IL-4 and IL-13 in BAT under both basal and cold stress conditions, although the up-regulation of IL-6 by adiponectin KO only occurred at room temperature condition, and the thermogenic marker PGC1α was only increased by adiponectin deficiency under cold stress conditions. n = 5–8/group. Data are presented as means ± SEM. *, P < 0.05; **, P < 0.01; Student's t test. GAPDH was used as an internal control. For the following studies, 15 d after first-time immunization of adiponectin KO and WT mice with papain and OVA, BALFs and LLNs were collected for the analysis. **(F)** The intracellular stain of Ki67 in LLNs ILC2s from adiponectin KO and WT mice after induction of experimental asthma. n = 6/group. Data are presented as means ± SEM. Student's t test. **(G)** Frequency of Th2 cells (TH2; Lin⁺CD4⁺GATA3⁺), ILC2s (Lin⁻CD4⁻GATA3⁺) and Th1 cells (TH1; Lin⁺CD4⁺IFNγ⁺) in LLN cells from adiponectin KO and WT mice after induction of experimental asthma. n = 6/group. Data are presented as means ± SEM. *, P < 0.05, Student's t test. **(H)** The intracellular stain of Ki67 in LLN Th2 cells, ILC2s, and TH1 cells from adiponectin KO and WT mice after induction of experimental asthma. n = 6/group. Data are presented as means ± SEM. **(I–L)** Student's t test. ELISA of inflammatory cytokines IL-4 (I), IL-5 (J), IL-13 (K), and IFNγ (L) released by LLN cells after ex vivo recall with OVA at indicated concentrations. n = 6/group. Data are presented as means ± SEM. *, P < 0.05; **, P < 0.01; Student's t test. **(M)** Cellular profile of BALFs from immunized adiponectin KO and WT mice. aMac, alveolar macrophages; Eos, eosinophils; iMac, inflammatory macrophages; Lym, lymphocytes; Mon, monocytes; Neu, neutrophils. n = 6/group. Data are presented as means ± SEM. *, P < 0.05; **, P < 0.01; Student's t test. ADPN, adiponectin.
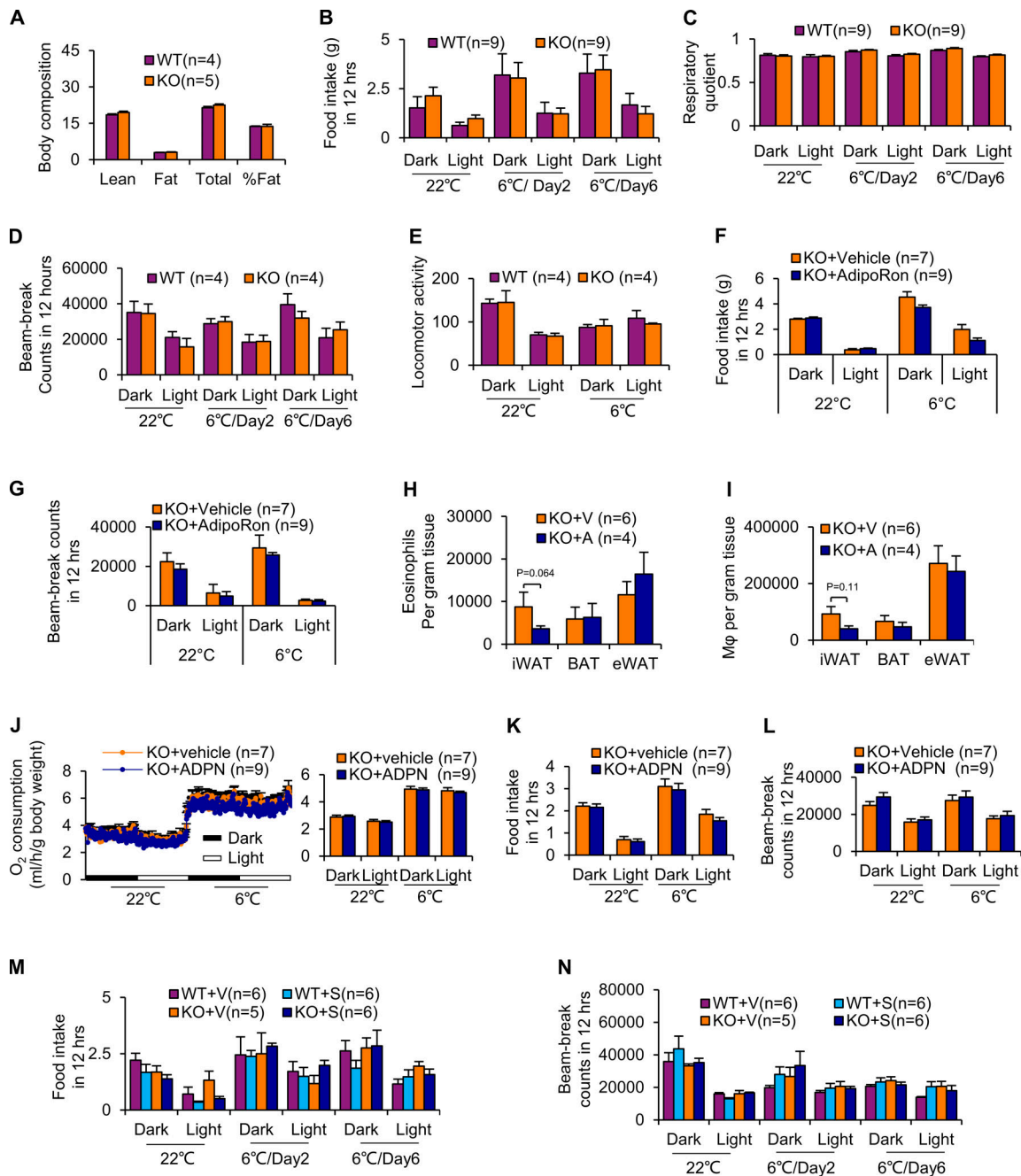
Figure S2. **Adiponectin inhibits thermogenesis in a peripheral tissue-dependent manner. (A–D)** For calorimetry analysis, mice were individually housed in the metabolic cages coupled with an environmental chamber. After 24-h adaptation at room temperature (22°C), the mouse was continuously housed in the system at 22°C for 48 h and then at 6°C for the times indicated. O_2 consumption, CO_2 release, food intake, body weight, water intake, break-beam activity, and wheel activity were monitored using the Sable International Phenotyping System. Given the difficulty in the balance of wheel activity and break-beam activity, the wheels were dissembled in the rest of studies. CO_2 release exhibited a same tenancy as O_2 consumption and was not included in the paper. The body composition (n = 4–5/group; A), food intake (n = 9/group; B), respiratory quotient (n = 9/group; C), and beam-break counts activity (n = 4/group; D) of adiponectin KO and WT mice at room temperature (22°C) and under cold stress condition (6°C) are shown. Data are presented as means ± SEM. Student's t test. **(E)** Locomotor activity of adiponectin KO and WT mice exposed to room temperature (22°C) and under cold stress conditions (6°C) with telemetry analysis. n = 4/group. Data are presented as means ± SEM. Student's t test. **(F and G)** The effect of AdipoRon administration on the food intake (F) and beam counts (G) of adiponectin KO and WT mice at room temperature (22°C) and under cold stress conditions (6°C). n = 7–9/group. Data are presented as means ± SEM. Student's t test. **(H and I)** AdipoRon treatment suppressed the frequency of eosinophils (H) and macrophages (I) in iWAT, but not BAT, in adiponectin KO mice under cold stress conditions. n = 4–6/group. Data are presented as means ± SEM. Student's t test. V, vehicle; A, AdipoRon. **(J–L)** O_2 consumption (J), food intake (K), and beam-break counts (L) of 10-wk-old male adiponectin KO mice that were administered with adiponectin by i.c.v. injection and housed at 22°C for 48 h and then at 6°C for 48 h. n = 7–9/group. Data are presented as means ± SEM. Student's t test. **(M and N)** Adiponectin KO and WT mice were administered with or without mouse ST2/IL-1 R4 antibody by i.p. injection, and food intake (M) and beam-break counts (N) of adiponectin KO and WT mice at room temperature (22°C) and under cold stress conditions (6°C) were measured. n = 5–6/group. Data are presented as means ± SEM. Student's t test. ADPN, adiponectin; S, ST2 antibody.
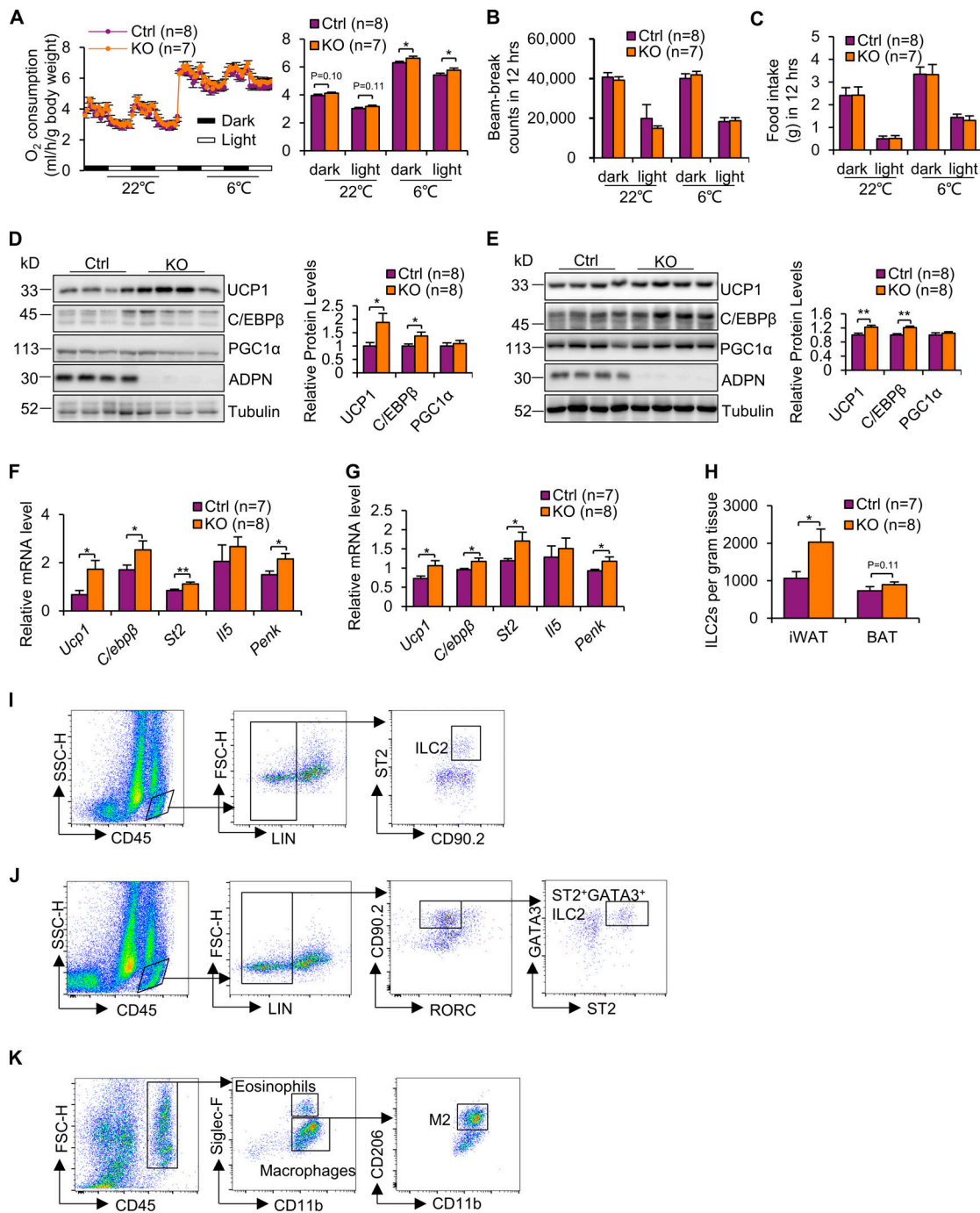
Figure S3. Adiponectin KO increased O₂ consumption and up-regulated thermogenic gene expression and ILC2 activation in adipose tissue of another mouse model (B6;129-Adipoqtm1Chan/J mice from Jackson Laboratory that were backcrossed with C57BL/6 mouse for four generations). (A–C) Adiponectin KO mice were individually housed for calorimetry analysis in the metabolic cages coupled with an environmental chamber. After 24-h adaptation at room temperature (22°C), mice were continuously housed in the system at 22°C for 48 h followed by cold exposure (6°C) for 48 h. O₂ consumption (A), beam-break activity (B) and food intake (C) were monitored at room temperature (22°C) and under cold stress conditions (6°C). The O₂ consumption data were normalized with body mass and analyzed by ANOVA. n = 7–8/group. Data are presented as means ± SEM. *, P < 0.05, Student's t test. **(D–G)** The expression levels of the thermogenic genes *Ucp1* and *C/ebpβ* in both protein and mRNA were significantly up-regulated in iWAT (D and F) and BAT (E and G) by adiponectin deficiency under cold stress conditions. The mRNA levels of the ILC2 markers *St2* and *Penk*, but not *Il5*, were significantly increased in iWAT (F) and BAT (G). n = 7–8/group. Data are presented as means ± SEM. *, P < 0.05; **, P < 0.01; Student's t test. **(H)** The population of ILC2s was increased by adiponectin KO in iWAT despite no significant effect in BAT under cold stress conditions. n = 7–8/group. Data are presented as means ± SEM. *, P < 0.05. Student's t test. For the flow cytometric analysis of adipose tissue, the gating strategy was summarized in the following figures (I–K). The SVFs from adipose depots were isolated from 10-wk-old male mice and used for the flow cytometry analysis. **(I)** CD45⁺Lin⁻CD90.2⁺ST2⁺ cells were applied on ILC2s for Fig. 1, A, B, E, and F; Fig. 2, B and C; Fig. 3, A and E; Fig. 5 D; Fig. 6 B; and Fig. S1 B. **(J)** CD45⁺Lin⁻CD90.2⁺RORC⁻ST2⁺GATA3⁺ cells were applied on ILC2s for Fig. S1 C. **(K)** Eosinophils (CD45⁺CD11b⁺Siglec-F⁺), macrophages (CD45⁺CD11b⁺Siglec-F⁻), and M2 macrophages (CD45⁺CD11b⁺Siglec-F⁻CD206⁺) were differentiated in SVF of adipose tissue. ADPN, adiponectin; FSC-H, forward scatter-height; SSC-H, side scatter-height.